Poster 1

MODELING THE THREE-DIMENSIONAL STRUCTURE OF THE YEAST NUCLEAR PORE COMPLEX

Frank Alber, Brian Chait, Julia Kipper, Mike Rout, Adisetyantari Suprapto, Whenzu Zhang, and Andrej Sali; The Pels Family Center for Biochemistry and Structural Biology, The Rockefeller University, New York, NY 10021

We calculated a 3D model of the yeast nuclear pore complex (NPC). The nucleoporin proteins are represented as spheres with the radii estimated from the lengths of their amino acid sequences. The NPC structure was obtained by minimizing violations of spatial restraints obtained from several sources. The restraints included exclusion volume restraints, protein-protein contact restraints extracted from approximately 30 immuno-purification experiments [1,2] and symmetry restraints. Symmetry restraints derived from cryo-electron microscopy [3] reproduce the 8 fold symmetry of the NPC complex. Each of the 8 symmetry units consist of 59 proteins. Starting with random configurations of NPC proteins, many 3D models were calculated by minimizing violations of the input spatial restraints, using a combined method of conjugate gradients and molecular dynamics with simulated annealing, as implemented in the program MODELLER[4]. The final configurations satisfying the input restraints well were clustered. The clusters were analysed to direct new experiments for obtaining maximum spatial information while minimizing the effort, and to address several outstanding questions in the structure-function relationship of the NPC.

[1] Rout, M.P., Aitchison, J.D., Suprapto, A., Hjertaas, K., Zhao, Y., Chait, B.T. "The Yeast Nuclear Pore Complex: Composition, Architecture, and Transport Mechanism" (2000) J. Cell. Biol. 148, 635-651.
[2] Chait,B.T, Kipper, J., Rout, M.P., Suprapto, A., Zhang, W., personal communication.
[3] Yang, Q., Rout, M.P., Akey, W. "Three-Dimensional Architecture of the Isolated Yeast Nuclear Pore Complex: Functional and Evolutionary Implications" (1998) Mol. Cell., 1, 223-224.
[4] Sali, A., Blundell, T.L. "Comparative protein modelling by satisfaction of spatial restraints" (1993) J Mol Biol 234, 779-815.

1) Royer, W.E., Strand, K., van Heel, M. and Hendrickson, W.A. (2000) Proc. Natl. Acad. Sci. 97, 7107-7111

Poster 2

MYOSIN HEAD DISPOSITION MODELED FROM LOW-ANGLE X-RAY DIFFRACTION OF RELAXED LETHOCERUS INSECT FLIGHT MUSCLE

Hind A. AL-Khayat[1], Liam Hudson[1], Michael K Reedy[2], Bruce Baumann[3], Thomas C Irving[4] & John M. Squire[1]; [1]Biological Structure and Function Section, Biomedical Sciences Division, Imperial College of Science, Technology & Medicine, London SW7 2AZ, UK, [2]Department of Cell Biology, Duke University, Durham, NC 27710, USA, [3]Florida State University, Tallahassee, FL, USA, 4Illinois Institute of Technology, Chicago, IL 60616, USA

Superbly ordered sarcomere structures in fibrillar insect flight muscle (IFM) and bony fish skeletal muscle favor detailed structural studies. We seek to picture the 3D molecular structures and actions of actin and myosin filaments in IFM by computer-modeling of low-angle X-ray patterns. Initially we are modeling IFM myosin head disposition to 5 nm resolution using the 1.43 nm resolution versions of both Rayment and Dominguez myosin heads crystal structures, and using 105 myosin reflections from MgATP-relaxed fibres of glycerinated IFM. We use the simulated annealing and local refinement approaches shown by Hudson et al. (J. Mol. Biol. 273: 440, 1997) to yield a 3% R-factor in their final best-fit-to-X-rays model of myosin head disposition on relaxed fish thick filaments. Our IFM model so far, based on layer lines 10, 16, 22, 26 and 32 (orders of 232 nm) has all crowns alike, all 8 [Rayment-type] heads per crown projecting at ~90° in a square shelf of density that rotates 33.75° for every 14.5 nm axial repeat. R-factor is 13.54%. Polarity re: Z- vs. M-band is clear from a unique fit to negative stained IFM thick filaments (Morris et al., J. Struct. Biol. 107: 237, 1991). Later, we propose to model the full unit cell, including thin filaments, against X-rays from relaxed, rigor and active IFM, ultimately to 1 nm resolution and study the interactions between the different proteins in the different muscle states.

Poster 3

BIOCHEMICAL PROBES OF MICROTUBULE STRUCTURE: THE FAST KINETICS OF TAXOL BINDING

José M. Andreu, I. Barasoain and J.Fernando Díaz . CIB, CSIC, Madrid, Spain

The accessibility of the Taxol binding site of microtubules has been investigated using kinetic methods. The kinetics of association of Taxol has been measured by competition with a specific fluorescent Taxol derivative (Flutax). The kinetic constant determined at 37 ºC with purified tubulin microtubules is k+ 3.6 ± 0.1 x106 M-1 s-1, 5 times faster than that of Flutax. Taxol binding is very similar to the first step of the reaction profile of Flutax binding (Díaz et al. 2000 JBC 275,26265-76), which probably corresponds to the binding of its Taxol moiety. The rate constant of Flutax binding depends on the solution viscosity as a diffusion controlled reaction. The fenestrations of the microtubule wall are too small for the fast entry of the taxoids.

Microtubule associated proteins (MAPs) moderately slow down the binding of Flutax. The taxol binding site in PtK2 microtubule cytoskeletons has been probed with Flutax. The observed kinetic rate constants of binding and dissociation are similar to MAP-containing microtubules. The available kinetic data clearly indicate that the Taxol binding site is fully exposed to the solvent. This suggests either that the inner microtubule face opens to the solvent in an extensive, presently unknown manner, or that the Taxol binding site is really at the outer microtubule surface.

Poster 4

ADVANCED INSTRUMENTATION FOR HIGH RESOLUTION ELECTRON CRYO-MICROSCOPY

B.L. Armbruster[1], K. Fukushima[2], M. Kawasaki[1], M. Kersker[1] and R. O'Donnell[1], [1]JEOL USA, Inc., Peabody, MA 01960, [2]JEOL Ltd., Akishima, Japan

In order to improve the quantity and quality of data collection, many laboratories are utilizing the advanced technology of intermediate voltage, field emission transmission cryoelectron microscopes operating at liquid helium temperatures. Large subcellular machines are directly examined in minutes by means of cryoTEM and rendered in three dimensions with a current resolution limit of 2Å. Dynamic events at the angstrom level are captured in milliseconds with rapid freezing of specific functional states, providing high-resolution detail and contextual structural information in the same image.

Helium microscopes have facilitated the structural analysis of two-dimensional arrays of membrane proteins such as light harvesting complex II, sodium channel, nicotinic acetylcholine receptor, aquaporin-1 and bacteriorhodopsin for reconstructions to 2.5?. The higher acceleration voltage of the microscope plus energy filtering permits viewing of thick-sectioned material for tomographic reconstructions. From cryoTEM data, processes of pharmcological significance such as the binding of taxol to tubulin monomers can be refined when compared to atomic models from x-ray crystallography.

Poster 5

ELECTRON TOMOGRAPHY OF HAIR CELL STEREOCILIA - TOWARD A 3D STRUCTURE OF THE HEARING MACHINERY

Manfred Auer[1,2], Bram Koster[3], Ulrike Ziese[3], Da Neng Wang[1] & A. James Hudspeth[2], [1]Skirball Institute, NYU Medical Center,
[2] Laboratory of Sensory Neuroscience, The Rockefeller University,
[3] University of Utrecht

The hair bundle of inner ear hair cells is responsible for detection of sound. Protruding from the apical cell surface, the bundle comprises dozens of stereocilia, which are cylindrical, actin-filled rods standing in a hexagonal array. When sound energy deflects a hair bundle the individual stereocilia slide along one another. This shearing motion is sensed by 'tip links', thought to be directly connected to mechanoelectrical transduction channels. Upon sustained stimulation, the hearing machinery adapts mechanically by adjusting the tension in the tip links via a movement of a nonconventional myosin along the actin filament bundle. We are studying the hearing machinery by electron tomography of resin-embedded sectioned sensory epithelia. Using progressive lowering of temperature dehydration, we have obtained unprecedented preservation quality. Alternatively, we can isolate individual stereocilia for vitrification. We have recorded several tomographic data sets of sectioned material. We have resolved the tip link protein, the actin filaments as well as certain globular densities that most likely represent the head domains of the non-conventional myosins. These myosins link the complex to the actin cytoskeleton and are suspected to be responsible for the adjustment of tip link tension between adjacent stereocilia. Our reconstruction represents the first true 3D image of the hearing machinery.

Poster 6

COMPUTATIONAL PREDICTION OF STRUCTURE-BASED DYNAMICS FOR BIOMOLECULAR COMPLEXES AND ASSEMBLIES

Ivet Bahar; Center for Computational Biology & Bioinformatics, and Department of Molecular Genetics & Biochemistry, School of Medicine, University of Pittsburgh, PA 15213, USA

Computational studies play an important role in structural genomics and proteomics initiatives, for predicting structures (Baker and Sali, 2001;Simons et al., 2001), target selection (Brenner, 2000), automated interpretation (Brunger et al., 1998) or integration (Bertone et al., 2001;Gerstein, 2000) of experimental data. With the determination of new structures, however, new questions arise. Of interest is to understand the dynamics of the new structures. A wealth of theoretical and experimental studies provide evidence for the close link between dynamics and function (Frauenfelder and McMahon, 1998;Stock, 1999). While conventional atomic resolution models and simulations can give insights about the conformational motions of biomolecules and the local dynamics near an active site, these approaches are severely hampered by time and memory limitations when larger scale or longer time processes are explored. New models and methods are needed for understanding the machinery of bio-macromolecular assemblies, or the cascades of interactions underlying particular cellular functions.

We have recently developed a new approach, called the Gaussian network model (GNM) for efficient characterization of the global dynamics of large molecules or complexes (Bahar et al., 1997;Bahar and Jernigan, 1998;Bahar et al., 1998; Bahar et al., 1999). The structure is modeled in this approach as a Gaussian network, the nodes of which represent the interaction sites that can be modeled at different resolutions, and the connectors are the intramolecular and intermolecular interactions maintaining the stability and functional flexibility of the structure. The GNM and its extensions are based on fundamental concepts of statistical mechanics applied to polymer networks (Flory, 1976) and methods of graph theory. The basic ingredient of the model is the contact topology, and the contacting elements or building blocks can be selected at different scales, ranging from individual residues to clusters comprised of large substructures. GNM thus can give insights about the collective dynamics relevant to function for structures determined at less than atomic resolution. Two important advantages of the GNM are its simplicity and its computational efficiency.

Our recent applications to large complexes, including the chaperonin GroEL-GroES complex (Keskin et al., 2001), tubulins (Keskin et al., 2002), influenza virus hemagglutinin A (Isin et al., 2002), indicate the utility and suitability of the approach for accurately predicting the allosteric communication mechanisms and domain movements controlling the function of large complexes. The approach seems to be particularly useful for investigating the cooperative dynamics of low resolution structures such as those determined by electron cryomicroscopy. Potential utility and applications of our computational approach for optimal modeling and analysis of multiprotein dynamics or networks of interactions at the subcellular level will be discussed.

References

1. Bahar,I., A.R.Atilgan, M.C.Demirel, and B.Erman. 1998. Vibrational Dynamics of Folded Proteins: Significance of Slow and Fast Motions in Relation to Function and Stability. Phys Rev Lett 80:2733-2736.

2. Bahar,I., A.R.Atilgan, and B.Erman. 1997. Direct evaluation of thermal fluctuations in proteins using a single- parameter harmonic potential. Fold. Des 2:173-181.

3. Bahar,I., B.Erman, R.L.Jernigan, A.R.Atilgan, and D.G.Covell. 1999. Collective motions in HIV-1 reverse transcriptase: examination of flexibility and enzyme function. J. Mol. Biol. 285:1023-1037.

4. Bahar,I. and R.L.Jernigan. 1998. Vibrational dynamics of transfer RNAs: comparison of the free and synthetase-bound forms. J. Mol. Biol. 281:871-884.

5. Baker,D. and A.Sali. 2001. Protein structure prediction and structural genomics. Science 294:93-96.

6. Bertone,P., Y.Kluger, N.Lan, D.Zheng, D.Christendat, A.Yee, A.M.Edwards, C.H.Arrowsmith, G.T.Montelione, and M.Gerstein. 2001. SPINE: an integrated tracking database and data mining approach for identifying feasible targets in high-throughput structural proteomics. Nucleic Acids Res. 29:2884-2898.

7. Brenner,S.E. 2000. Target selection for structural genomics. Nat. Struct. Biol. 7 Suppl:967-969.

8. Brunger,A.T., P.D.Adams, and L.M.Rice. 1998. Recent developments for the efficient crystallographic refinement of macromolecular structures. Curr. Opin. Struct. Biol. 8:606-611.

9. Flory,P.J. 1976. Statistical Thermodynamics of Random Networks. Proc. Roy. Soc. Lond. A. 351:351-380.

10. Frauenfelder,H. and B.McMahon. 1998. Dynamics and function of proteins: The search for general concepts. Proc. Natl. Acad. Sci (USA) 95:4795-4797.
11. Gerstein,M. 2000. Integrative database analysis in structural genomics. Nat. Struct. Biol. 7 Suppl:960-963.
12. Isin,B., P.Doruker, and I.Bahar. 2002. Functional motions of influenza virus hemagglutinin. A structure-based analytical approach. Biophys. J. in press..
13. Keskin,O., I.Bahar, D.Flatow, D.G.Covell, and R.L.Jernigan. 2001. Molecular mechanisms of chaperonin GroEL-GroES function. Biochemistry in press.
14. Keskin,O., S.R.Durrell, I.Bahar, R.L.Jernigan, and D.G.Covell. 2002. Relating molecular flexibility to function. A case study of tubulin. Biophys. J. in press.
15. Simons,K.T., C.Strauss, and D.Baker. 2001. Prospects for ab initio protein structural genomics. J. Mol. Biol. 306:1191-1199.
16. Stock,A. 1999. Relating dynamics to function. Nature 400:221-222.

Poster 7

STRUCTURAL AND FUNCTIONAL MINING OF INTERMEDIATE RESOLUTION STRUCTURES OF BIOLOGICAL MACHINES

Matthew Baker, Wen Jiang and Wah Chiu; Department of Biochemistry and Molecular Biology, Baylor College of Medicine, Houston, Texas 77030

While large macromolecular machines are often difficult to study by current high-resolution structural techniques, advancements in electron cryomicroscopy have made the elucidation of these large structures at intermediate resolutions (~6-12 Å) possible. At this resolution, significant structural information can be obtained from a rigorous analysis of the structure, but in general is complicated and subjective. In an effort to overcome this, we have developed a methodology to computationally extract additional structural and functional features from an intermediate resolution structure, which is then integrated with bioinformatics and traditional biochemistry. At the core of this methodology are two novel structural feature recognition programs, helixhunter and foldhunter, which can identify helices and homologous sub-structures, respectively, within these large complexes. In applying this methodology to three specific projects, we have been able to identify, localize and characterize a previously unknown functional domain in the skeletal muscle Ca^{2+} release channel (~2.4 MDa), identify key structural motifs in different domains of the major capsid protein of Herpes Simplex Virus-1 (~200 MDa) and deduce the entire three-dimensional protein folds for two capsid proteins of the Rice Dwarf Virus (~50 MDa). This structural data mining procedure has proven to be an attractive methodology to maximize the information content from an intermediate resolution structure of large macromolecular machines.

Poster 8

TOWARDS STRUCTURE DETERMINATION OF MEMBRANE PROTEINS IN 2-DIMENSIONAL CRYSTALS USING NEXT-GENERATION HARD X-RAY SOURCES.

Michael Becker; Biology Dept., Brookhaven National Laboratory, P.O. Box 5000, Upton, NY 11973

It has been proposed that hard X-Ray Free Electron Lasers, such as the Linac Coherent Light Source (LCLS) planned for development at Stanford, may be useful for structure determination of membrane proteins in 2-D crystals [1, 2]. More recently, several proposals to develop Energy Recovery Linacs, such as the Photoinjected Energy Recovery Linac (PERL) planned for development at Brookhaven, have been put forth. Both types of future X-Ray sources are expected to provide hard X-Rays pulses that are ultrashort (about 100 to 200 fs in pulse width) and ultrabright (orders of magnitude brighter than from current sources); these characteristics are essential for high-resolution structure determination of 2-D samples. Appropriate sample preparation will likely be the main practical difficulty in realizing the stated goal. It is expected that 2-D X-Ray experiments will be highly complementary to electron-microscopy experiments. Application of pulsed X-Ray techniques to large macromolecular complexes in 2-D crystals, whether the complexes are membrane-integral or water-soluble, may be fruitful.

1) Becker, M. (1999) Biophysical Journal 76, A121.
2) Becker, M. (1999) "Transparencies from the EMBO Workshop: Potential Future Applications in Structural Biology of an X-Ray Free Electron Laser at DESY", EMBL, Hamburg, pp. 184-198.

Poster 9

SENSITUS–FORCE FEEDBACK FOR FITTING EM AND X-TAL DATA

Stefan Birmanns[1] , Willy Wriggers[2]; [1]Central Institute for Applied Mathematics, Research Centre Juelich, Germany, s.birmanns@fz-juelich.de; [2]Department of Molecular Biology, The Scripps Research Institute, wriggers@scripps.edu

SenSitus is a tool for interactive fitting of high-resolution crystal structures into low-resolution maps from electron microscopy. SenSitus supports the fitting process by the use of a force feedback device. The force feedback device not only enables the user to position the structure in the 3D space, but also guides the manual fitting. The program achieves this by calculating forces according to the correlation coefficient of the maps and crystal data. This technique is very useful, it makes it easier to detect possible fitting locations and simplifies the fine positioning of the structure.

We are using the Phantom force feedback devices (6DOF and 3DOF) from SensAble Corp. The device measures a user's hand position and exerts a precisely controlled force on the hand.

The program visualizes the PDB and EM files by the help of 3D graphics, using virtual reality techniques. It can be run in VR environments like VR workbenches or CAVEs, but can also be used on standard workstations. It has an intuitive GUI and is very portable (Linux, IRIX and Windows versions are available).

Poster 10

CONFORMATIONAL CHANGES IN THE NUCLEOTIDE BINDING DOMAIN OF THE ABC TRANSPORTER RbsA DUE TO ATP HYDROLYSIS

Matthew C. Clifton ‡, Huide Zhang §, Shelly Armstrong ‡, Mark A. Hermodson §, Cynthia Stauffacher ‡; From the ‡Department of Biological Sciences and the §Department of Biochemistry, Purdue University, West Lafayette, Indiana 47906.

Energy-dependent transport of molecules across the membrane is an essential process for the cell and has been implicated in a number of diseases. To gain an understanding of the mechanism of energy-dependent transport, our laboratory has been investigating the ribose transport system from E.coli. The ribose transport complex from E.coli contains a membrane-spanning domain, RbsC, and RbsA, which is composed of two ATPase domains. The structure of the N-terminal half of RbsA containing ADP and magnesium was solved to 1.6 Å by MIR phasing. The crystals have P212121 symmetry with a=46.5 Å, b=57.7 Å, and c=108.5 Å. Work is now in progress to obtain the structure of RbsA with the non-hydrolyzable ATP analog AMPPNP bound. The new crystals display orthorhombic symmetry, but display neither the same space group or unit cell parameters. Phases therefore could not be obtained directly and are being obtained using molecular replacement. These two structures will allow an investigation of potential changes in the structure of RbsA due to ATP hydrolysis.

Poster 11

TOWARDS ATOMIC RESOLUTION STRUCTURES OF TYPE IV PILI

L. Craig[1], A. S. Arvai[1], R. K. Taylor[2], M. Pique[1], M. Singh[3], D.S. Shin[1], B. D. Adair[4], S. J. Lloyd[1], K. T. Forest[5], M. Yeager[4] and J. A. Tainer[1]; [1]The Scripps Research Institute, Dept. of Molecular Biology and [4]Dept. of Cell Biology, La Jolla, CA; [2]Dartmouth Medical School, Dept. of Microbiology, Hanover, NH; [3]Albert Einstein College of Medicine, Bronx, NY; [5]University of Wisconsin, Department of Bacteriology, Madison, WI

We are working towards high resolution structures of type IV pili by combining xray crystallography of the pilin subunits with cryo-EM and 3D image reconstruction of the assembled fibers. Type IV pilins are defined by several common features: a highly-conserved 60 amino acid N-terminus; a C-terminal disulfide bridge; an N-methylated N-terminus; and a common assembly machinery. We have solved the crystal structures of type IV pilins from three different pathogens and shown that they also have a conserved overall structure, with an extended N-terminal α-helix and an anti-parallel four-stranded β-sheet comprising much of the C-terminus. We hypothesize that type IV pili share a common mode of assembly with the N-terminal α-helices forming a hydrophobic core and the β-sheets wrapping around the fiber. We are constructing a fiber model based on the crystal packing arrangement of *V. cholerae* pilin, which exist in a helical fiber-like arrangement. We have been using cryo-EM and single particle methods to determine the helical repeat of the fiber. However, due to the extreme smoothness of the fibers only two fibers of the hundreds we have analyzed reveal any structural information. We are planning to decorate the surfaces of the pili by gold or immunolabelling and will apply the automated acquisition program LEGINON to the frozen pili. We will use the helical image reconstruction program PHOELIX to derive low resolution electron density maps of pilus filaments, which will provide a molecular envelope for docking the pilin subunit structures, thereby generating pseudo-atomic resolution models of intact pili.

Poster 12

CYANOBACTERIAL PHOTOSYSTEM II AND ITS ANTENNAE SYSTEM

Paula C. A. da Fonseca, Edward P. Morris & James Barber; Biochemistry Department, Imperial College, London SW7 2AY, U.K.

Photosystem II (PSII) is the photosynthetic transmembrane protein-pigment complex which utilises light energy to drive the splitting of water and release of oxygen, a unique reaction in biological systems. We determined a Synechococcus elongatus PSII core projection map, at a resolution of 16Å, by image processing of two-dimensional crystals formed by in vitro reconstitution. The analysis of this map and its comparison with a 10Å three-dimensional map recently obtained by electron crystallography of the closely related higher plant PSII core dimer indicates a similar organisation of the main transmembrane domains. Moreover, differences were identified which can be related to the content and organisation of the small transmembrane subunits and extrinsic proteins of the PSII complex in each organism. These data on the structure of cyanobacterial PSII core was also used to understand its interaction with the external antennae complex, the hydrophilic phycobilisomes. Although some models have been suggested, the molecular interactions and the mechanisms of energy transfer between the phycobilisome core and PSII are far from fully understood. We analysed the Synechococcus elongatus phycobilisome core complex by single particle analysis and we combined the map obtained with the structural data on the PSII complex in order to build up a model of a phycobilisome core-PSII supercomplex. From this model we proposed interaction domain between the two complexes.

Poster 13

CRYO-ELECTON MICROSCOPY OF VITREOUS SECTIONS: CELL ULTRASTRUCTURE REVISITED.

Jacques Dubochet, Laboratory for Ultrastructural Anlaysis, University of Lausanne, CH-1015 Lausanne, Switzerland and Alasdaidre McDowall, Centre for Microscopy and Microanalysis, University of Queensland, St. Lucia, QLD 4072 Australia.

The cell is a dynamic body functioning under non-equilibrium conditions. However, at the ultrastructural level (2nm - 200 nm) and at the time scale between 10-3 and 102 sec, most of our knowledge relies on observations made on slowly fixed and dehydrated material. Could it be that our view of the cell is therefore misguided?

Cryo-electron microscopy of vitreous hydrated sections is an obvious method for answering this question. It consists in vitrifying a sample of native tissue by ultra-rapid cooling, cutting it into thin cryo-sections and to observe the sections directly in the cryo-electron microscope without fixation, staining and dehydration. The method has long been hampered by technical difficulties but important progress has been made recently in the areas of cooling under high pressure, and in cryo-sectioning.

As it was shown for thin layers of vitrified biological suspensions 20 years ago, we have found that vitreous sections can reveal the finest details of the cell. Often the region of interest is structurally superior to conventionally fixed and stained preparations. What is observed is often very different from knowledge gained from conventional techniques. One major remaining problem is that the amount of structural information within the thickness of a 70nm - 100nm vitreous section is generally too large and complex for easy interpretation. Undoubtedly the future lies in combining cryo-sections with electron tomography and computer image reconstruction.

Poster 14

STRUCTURE OF A BACTERIAL DNA-PROTEIN COMPLEX THAT MEDIATES NUCLEAR IMPORT IN PLANTS

Michael Elbaum[1], Asmahan Abu-Arish[1], Sharon Grayer Wolf[2]
[1]Dept of Materials and Interaces and [2]Electron Microscopy Center, Weizmann Institute of Science, Rehovot, Israel

Agrobacterium tumefaciens infects plant cells by transfer of a linear single-stranded DNA plasmid containing tumor-inducing genes. It represents the only known example of genetic transfer across living kingdoms, and is similar to certain viral nucleocapsids. A natural pathogen, it has developed into a major tool for plant genetic engineering. Two bacterial proteins are primarily responsible for packaging the DNA in preparation for import to the host cell nucleus: VirD2 cuts and binds to the transfer DNA at a sequence-specific border site, and VirE2 binds stoichiometrically along the length of the DNA strand. The resulting helical complex has dimensions suitable for passage through the plant nuclear pores. We are analyzing the three-dimensional structure of this VirE2-ssDNA complex using helical reconstruction and single-particle methods. Although no crystal structure of VirE2 is yet available, our preliminary results indicate a three-domain structure for the protein, consistent with earlier mutation analyses. The exposed surface of the complex binds plant factors that activate, and thus co-opt, the protein nuclear import machinery in the host cell. The simplicity and regularity of the VirE2-ssDNA complex will enable a new look at the structure of the nuclear pore during active translocation.

Poster 15

COMPARATIVE PROTEIN STRUCTURE MODELS FOR MOLECULAR MODELING OF THE YEAST RIBOSOME

N. Eswar[1], C.M.T. Spahn[2], R. Beckmann[3,4], P.A. Penczek[5], G. Blobel[3], J. Frank[2,6], A. Sali[1]; [1]Laboratory of Molecular Biophysics, Pels Family Center for Biochemistry and Structural Biology, The Rockefeller University, New York, NY 10021; [2]Wadsworth Center, Howard Hughes Medical Institute, Empire State Plaza, Albany, New York 12201; [3]Laboratory of Cell Biology, Howard Hughes Medical Institute, The Rockefeller University, New York, NY 10021; [4]Institut für Biochemie der Charité, Humboldt Universtität zu Berlin, Monbijoustr. 2, 10117, Berlin, Germany.; [5]University of Texas, Houston Medical School, 6431 Fannin, Houston, Texas 77030; [6]Department of Biomedical Science, State University of New York at Albany, Albany, New York 12222.

While cryo-electron microscopy (EM) and x-ray crystallography allow us to determine atomic resolution structures of large macromolecular assemblies, this process is time consuming. Fortunately, the structures of large assemblies and their constituent parts tend to be conserved in evolution, enabling homology protein structure modeling to enhance the value of low-resolution electron density maps. To illustrate this point, we present here the fitting of homology models for the yeast ribosomal proteins into a low-resolution cryo-electron density map of the whole yeast ribosomal particle.

High-resolution crystallographic structures are available for the archaeal ribosomes, but not for the eukaryotic yeast ribosome. However, there is a 15Å cryo-EM map for the yeast ribosome [1].

While there are species-to-species variations in the ribosome size and protein/RNA ratio, evolutionary conservation of rRNA and ribosomal proteins indicates similar quaternary structure among the archaeal and eukaryotic ribosomes. An automated software pipeline for comparative modeling, ModPipe [2], produced comparative models for 43 out of the 77 proteins of the yeast ribosome, based on their archaeal homologs of known 3D structure [3]. The models were calculated using alignments with sequence identities from 20 to 56% (an average of 32%) and e-values better than 10^{-4}. The modeled fraction of the yeast ribosomal sequences ranges from 34 to 99% (an average of 75%). The models were docked manually into the cryo-EM density with the aid of the program O [4]. Thus, a combination of EM and homology modeling resulted in a partial molecular model of the whole ribosomal particle. Future efforts may focus on automating the entire procedure by generating a spectrum

of homology models (based on alternate alignments, templates, domain orientations, etc.) and using automated docking methods to fit the models into the electron density data.

References:

1. Beckmann R, Spahn CM, Eswar N, Helmers J, Penczek PA, Sali A, Frank J, Blobel G: Architecture of the Protein-Conducting Channel Associated with the Translating 80S Ribosome. Cell 2001, 107:361-372.

2. Sanchez R, Sali A: Large-scale protein structure modeling of the Saccharomyces cerevisiae genome. Proc.Natl.Acad.Sci.U.S.A 1998, 95:13597-13602.

3. Spahn CM, Beckmann R, Eswar N, Penczek PA, Sali A, Blobel G, Frank J: Structure of the 80S Ribosome from Saccharomyces cerevisiae-tRNA- Ribosome and Subunit-Subunit Interactions. Cell 2001, 107:373-386.

4. Jones TA, Zou JY, Cowan SW, Kjeldgaard: Improved methods for binding protein models in electron density maps and the location of errors in these models. Acta Crystallogr.A 1991, 47 (Pt 2):110-119.

Poster 16

CRYSTALLOGRAPHIC STUDIES OF DEDD FAMILY EXORIBONUCLEASES

Tristan J. Fiedler & Arun Malhotra; Department of Biochemistry & Molecular Biology, University of Miami School of Medicine, Miami, FL 33101, USA

Ribonucleases play a central role in vital cellular processes such as mRNA degradation and maturation of stable RNAs. Eight distinct exoribonucleases have been identified in *E. coli*. Of these, three (RNase T, RNase D, & oligoribonuclease) are members of a larger exonuclease superfamily (named the DEDD exonuclease family, after the four invariant acidic residues in these proteins) that includes the proof-reading domains of DNA polymerases.

While these proteins share similar sequence motifs, they are functionally quite different. RNase T is involved in tRNA turnover and maturation of tRNAs, 23S, & 5S rRNAs. RNase D is also involved in tRNA maturation, but mainly as a backup enzyme. RNase D functions as a monomer, while RNase T and oligoribonuclease exist as dimers. Oligoribonuclease catalyzes the degradation of very short RNAs, and is the only exoribonuclease essential for cell viability.

We have initiated crystallographic studies of bacterial exoribonucleases, in collaboration with the laboratory of Dr. Murray Deutscher at the University of Miami. Crystals of oligoribonuclease have been obtained and we will present a structure for this protein, currently being modeled using experimental MAD phases extending to 2.2 Å. The long term goals of this research are to understand the structures and mechanisms of action of all exoribonucleases in a single organism; these studies complement a parallel study, underway in the Deutscher Laboratory, to characterize the physiological role of all the exoribonucleases in *E. coli*.

Poster 17

STRUCTURE OF A STATHMIN-LIKE DOMAIN : TUBULIN COMPLEX.

Benoît Gigant[a], Patrick A. Curmi[b], Carole Martin-Barbey[a], Raimond Ravelli[c], André Sobel[b] and Marcel Knossow[a]; [a]LEBS, CNRS Gif sur Yvette, France [b]INSERM U 440 Paris, France [c]EMBL Grenoble, France

To fulfill their functions microtubules assemble and disassemble continuously regulated by several families of proteins, among which the stathmin family. Stathmin family proteins share a domain which binds to tubulin in a 2 tubulin:1 stathmin-like domain ternary complex. The structure of the tubulin molecules of the complex was determined by Molecular Replacement. The current model of the structure, consisting of a stahmin α-helix and two tubulin molecules, has been refined to an R-factor of 27% at 4Å. More recently, in a peak-SAD experiment, three Seleno-methionine residues (out of ca 2100 residues in the complex) were located in the stathmin-like α-helix and allow a preliminary assignment of its sequence.

The structure reveals a complex made of a curved head-to-tail assembly of two tubulin molecules, maintained by the stathmin-like α-helix that runs all along it. The tubulin residues that contact stathmin in the complex are identical in the two αß heterodimers. Most interestingly, the spacing along the stathmin-like sequence of the residues that contact tubulin is identical to the spacing of corresponding residues in an internal sequence duplication found in all stathmin family proteins. This strongly suggests that stathmin family proteins have evolved to bind two tubulin molecules and that this is their main function in the cell. The mechanism of action of stathmin will be discussed.

Poster 18

ELECTRON TOMOGRAPHY OF WHOLE CELLS AND ORGANELLES

Grant Jensen[1], Dieter Typke[1], Julia Kuerner[2], Tina Weatherby[3], and Kenneth Downing[1]; [1]Lawrence Berkeley National Lab, [2]Max Planck Institute for Biochemistry; [3]University of Hawaii Manoa

Electron tomography is an emerging technology that can reveal the three-dimensional structures of unique objects such as whole cells, organelles, or short-lived macromolecular complexes to medium resolutions (~5 nm). It can be performed on plastic-embedded sections as well as thin films of frozen-hydrated specimens. We report initial tomographic studies of a plastic-embedded, sectioned, and stained microtubule bundle from copepod mechanoreceptors wherein individual microtubules are clearly resolved. We also report initial tomographic studies of a complete, frozen-hydrated "minimal" cell, Mesoplasma florum, that resolve individual, intracellular, ribosome-sized particles. State-of-the-art instrumentation now being installed is expected to allow "molecular resolution" tomograms wherein large macromolecular complexes will be identifiable within their native, intracellular environment.

Poster 19

THREE-DIMENSIONAL STRUCTURE OF IP_3 RECEPTOR CHANNEL AT 24 Å RESOLUTION

Qiu-Xing Jiang, Edwin C. Thrower, David W Chester, Barbara E. Ehrlich and Fred J. Sigworth, Departments of Cellular and Molecular Physiology and Pharmacology, Yale University, 333 Cedar Street, New Haven, CT 06520

We report here the first three-dimensional structure of type 1 inositol 1,4,5-trisphosphate receptor. Cryo-electron microscopic images of purified receptors in detergent micelles were obtained in the presence of EGTA. A 3D structure was synthesized by single particle reconstruction. The 24 Å resolution model takes the shape of an uneven dumbbell, and is ~170 Å tall. Its larger end is quite bulky and has four bodies protruding laterally by ca. 50 Å, which makes it presumably the cytoplasmic domain. The smaller end has structural features to be the transmembrane domain. The model has a largest lateral dimension of approximately 155 Å from one protruding body to the neighboring one, and is approximately 120 Å at the luminal side of the transmembrane domain. The two domains join at a low density region. The cavities enclosed in the transmembrane domain and the cytoplasmic domain may form a central vestibule for ion flux when the channel opens. The structure of IP3 receptor is quite different from that of the other calcium release channel–the ryanodine receptor.

Poster 20

TOWARDS HIGH THROUGHPUT AND HIGH RESOLUTION 3-D SINGLE PARTICLE RECONSTRUCTION OF MACROMOLECULAR COMPLEXES

Wen Jiang and Wah Chiu; Verna and Marrs McLean Department of Biochemistry and Molecular Biology, Baylor College of Medicine, Houston, TX 77030

Electron cryomicroscopy of large macromolecular complexes is becoming an increasingly powerful tool for revealing three-dimensional structures without the need for crystallization. The execution of image processing, however, requires experience and is error prone due to the need for a human operator to carry out interactive and repetitive processes. We have designed a computational environment, which is intended to use well-established image processing programs and to glue them together so that the lengthy and tedious data processing steps can be easily used by both experts and inexperienced investigators. This environment should also allow the incorporation of new algorithms and facilitate the management of the increasingly large data sets of single particles needed to achieve higher resolution reconstruction. To demonstrate this approach, we have implemented Semi-Automated Virus Reconstruction (SAVR), an expert system that integrates the most CPU intensive and iterative steps for icosahedral particle reconstruction using the scripting language Python. SAVR is portable across platforms and has been parallelized to run on both shared and distributed memory platforms. The package has been successfully applied to several data sets to generate icosahedral reconstructions to sub-nanometer resolutions (7-10 Å). For instance, we were able to complete a 3-D structure of phage P22 procapsid shell to 8.5 Å with ~12,000 particles in less than 2 weeks. This structure reveals clearly the locations of helices and beta sheets. This approach is being extended for reconstruction of single particles with any or no symmetry towards atomic resolution.

Poster 21

CONTRAST TRANSFER FUNCTION—ESTIMATION OF PARAMETERS

Laurent Joyeux, Pawel A. Penczek; Department of Biochemistry and Molecular Biology; University of Texas–Houston Medical School, 6431 Fannin, Houston, TX 77030, USA.

In single particle analysis, the selection of individual particle views from micrographs is a time consuming and repetitive task. A number of computational procedures with various degrees of automation have been developed in order to streamline this process and to reduce the operator's involvement. Since the quality of micrographs varies and they contain many features that can be easily mistaken for particle views, no consensus method of particle picking emerged yet. Some of the existing methods are based on edge detection, other employ template matching methods. We proposed a strategy that comprises two stages. In the first stage, initial selection of particles is performed based on a pyramid structure of gradually reduced in size and resolution versions of a micrograph. The upper levels of the pyramid are used to progressively reject false objects and other areas of a micrograph too large to correspond to particles. The lower levels are used to correct particle detection decisions made on higher levels. In the second stage of the procedure, the selected areas are identified using either statistical classification methods, or, in case reference structure is available, using template matching techniques. In the latter case, the Synthetic Discriminant Functions are employed.

Poster 22

PURIFICATION AND STRUCTURAL ANALYSIS OF NATIVE INTERMEDIATE-CONTAINING SPLICEOSOMES

Melissa S. Jurica, Melissa J. Moore, Nikolaus Grigorieff; Howard Hughes Medical Institute/ Biochemistry Department, Brandeis University, Waltham, MA

Pre-mRNA splicing takes places within the spliceosome, a dynamic macromolecular machine assembled from snRNP subunits containing both RNAs and proteins, and additional splicing factors. There has been much progress in elucidating the biochemical mechanisms required to complete a round of intron excision and exon ligation. However, little 3-D structural information is available for spliceosomes at any step of assembly. We purified spliceosomes assembled in vitro on an affinity-tagged pre-mRNA substrate. The pre-mRNA carries a 3' splice site mutation that efficiently accumulates spliceosomes containing splicing intermediates. These purified complexes contain U2, U5 and U6 snRNAs, as expected for this step of assembly. Mass spectrometry confirms the presence of core snRNP proteins, U2 and U5 snRNP specific proteins, as well as second step factors. Images of these spliceosomes in negative stain reveal particles with dimensions of approximately ca. 270 x 240 angstroms that assort into well-defined classes. We used angular reconstitution to calculate an initial 3-D structure from approximately 4000 negatively-stained single particle images assorted in 50 class averages. This structure reveals a particle with a remarkable open arrangement of large domains. Currently we pursuing structural analysis under cryo-conditions.

Poster 23

EXAMINING THE ALPHA-ACTININ-b1-INTEGRIN STRUCTRUAL RELATIONSHIP USING CRYO-EM

Debbie Kelly, Dianne Taylor, Kenneth A. Taylor
Institute of Molecular Biophysics, Florida State University, Tallahassee, FL 32306

Our interest lies in visualizing adhesive assemblies of structural proteins that anchor actin filaments to the cytoplasmic side of the fibronectin receptor, the β1-integrin. We have synthesized the integrin cytoplasmic domain with a histidine-tag at its N-terminus, which binds to a lipid monolayer containing a nickel-chelating group. This orientation is intended to mimic the native conformation at the cytoplasmic leaflet. A nano-gold particle was covalently linked to an additional C-terminal cysteine on the integrin, and co-crystallized with chicken gizzard alpha-actinin. We examined frozen-hydrated crystals of the integrin-alpha-actinin complexes, with and without gold-label, using Cryo-EM. 2D projections were calculated for each, along with a difference map to determine the relative position of the integrin. A statistical t-test ($p < 0.005$) indicates the significance of the electron density attributed to the nano-gold label. The 2D maps reveal that the β1-integrin binds alpha-actinin between the first and second, three-helix motifs asymmetrically in the central rod domain, which is in agreement with it's biochemical characterization.

Poster 24

ELASTIC CONFORMATIONAL TRANSITIONS

M. K. Kim[1], G. S. Chirikjian[1], Robert L. Jernigan[2]; [1]Department of Mechanical Engineering, The Johns Hopkins University, Baltimore, MD 21218; [2]Laurence H. Baker Center for Bioinformatics and Biological Statistics, Iowa State University, Ames, IA 50011-3020

We have developed a computationally efficient and physically realistic method to simulate the transition of a macromolecule between two conformations. Our method is based on a coarse-grained elastic network model in which contact interactions between spatially proximal parts of the macromolecule are modeled with Gaussian/harmonic potentials. To delimit the interactions in such models, we introduce a cutoff to the permitted number of nearest neighbors. This generates stiffness (Hessian) matrices that are both sparse and quite uniform, hence allowing for efficient computations. Several toy models are tested using our method to mimic simple classes of macromolecular motions such as stretching, hinge bending, shear, compression, ligand binding and nucleic acid structural transitions. Simulation results demonstrate that the method developed here reliably generates sequences of feasible intermediate conformations of macromolecules, since our method observes steric constraints and produces monotonic changes to virtual bond angles and torsion angles. Application has been made to the opening process of the protein lactoferrin, and because coarse graining is feasible, we are applying it to the transition of viral capsid structures. Below is an example of ligand binding, where both partners deform to admit the ligand.

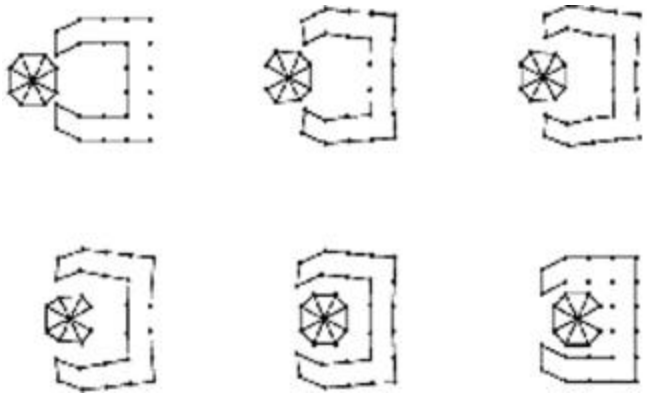

Poster 25

OPTIMIZING THE FIT OF KNOWN STRUCTURES INTO ELECTRON MICROSCOPE IMAGES

Andrei Korostolev, Lifan Chen, Jinghua Tan, Ken Taylor, Felcy Fabiola, Eric Blanc & Michael S. Chapman; Department of Chemistry & Biochemistry, Department of Biological Science and Institute of Molecular Biophysics, Florida State University, Tallahassee, FL 32306-4380

Real-space refinement methods have been adapted for the fitting of rigid fragments of known structures into the electron density from a variety of types of electron microscope images. Real-space refinement involves the optimization of the agreement between density calculated from the atomic model, and that observed experimentally. It therefore differs from conventional crystallographic refinement which is performed in reciprocal space, by optimizing the agreement between observed and calculated structure amplitudes.

The refinement was first developed as a crystallographic method [1] for application at about 3 Å resolution. It has now been applied successfully to electron microscopic images between 12 and 70 Å resolution. Techniques to which it has been applied include single particle reconstruction from cryo-EM data, with and without icosahedral symmetry, and both stained and unstained electron tomographic images [2].

Core to the method is the calculation of the expected electron density (and its positional derivatives) from the current model. In contrast to prior methods, this is calculated by Fourier transformation of the atomic scattering factors, truncated at the experimental resolution limits. Support, specific to electron microscopy, includes electron scattering factors, and (limited) corrections to the transfer contrast function that can be applied isotropically in reciprocal space.

RSRef was programmed as a refinement target to be used in other refinement packages. The distributed implementation is a module for TNT [3] that supports optimization by conjugate gradient methods. We are currently porting the EM module to CNS [4]. The parent programs support the application of full stereochemical restraints. In our refinement of acto-myosin complexes, the proteins were each treated as 1 to 4 rigid fragments separated by restrained hinge-points. In this case the primary effect was to resolve 70% of the poor contacts while retaining the good fit to the density of the initial model. A refinement of a ribosome structure,

in collaboration with Haixiao Gao and Joachim Frank improved both the fit to the density and the non-bonded contacts.

1. Chapman, M.S., Restrained Real-Space Macromolecular Atomic Refinement using a New Resolution-Dependent Electron Density Function. Acta Crystallographica, 1995. A51: p. 69-80.
2. Chen, L.F., E. Blanc, M.S. Chapman, and K.A. Taylor, Real space refinement of acto-myosin structures from sectioned muscle. J Struct Biol, 2001. 133(2-3): p. 221-32.
3. Tronrud, D.E., L.F. Ten Eyck, and B.W. Matthews, An Efficient General-Purpose Least-Squares Refinement Program for Macromolecular Structures. Acta Crystallographica, 1987. A43: p. 489-501.
4. Brünger, A.T., P.D. Adams, G.M. Clore, P. Gros, R.W. Gross-Kunstleve, J.-S. Jiang, J. Kurzewski, M. Nilges, N.S. Pannu, R.J. Read, L.M. Rice, T. Simonson, and G.L. Warren, Crystallography and NMR system: A new software system for macromolecular structure determination. Acta Crystallographica, 1998. D54: p. 905-921.

Poster 26

FAST ROTATIONAL MATCHING

Julio A. Kovacs, Pablo Chacon, Willy Wriggers; The Scripps Research Institute, Dept. of Molecular Biology, TPC-6, 10550 N. Torrey Pines Rd., La Jolla, CA 92037, jkovacs@scripps.edu, pchacon@scripps.edu, wriggers@scripps.edu

We present a computationally efficient method -'Fast Rotational Matching' or FRM- for performing rigid body docking of macromolecular structures over different levels of resolution. This method uses a new parametrization of the 3D rotation group, which makes it possible to efficiently compute the Fourier transform of the rotational correlation function. Then an inverse FFT gives the rotational correlation function itself. Previous methods have used Fourier techniques for the translational correlation function, but the rotations were determined by exhaustive search. Preliminary tests show that FRM is roughly three orders of magnitude faster than the exhaustive rotational search. This would make it adequate for interactive docking sessions, reducing computation times from hours to seconds. Another advantage of this method is the fact that it is not affected by possible differences of scale between the structures to be docked.

FRM is currently being tested in the docking of protein structures into low-resolution electron microscopy maps, and a slight variant of it will be applied to the protein-ligand docking problem, of importance in drug design.

Poster 27

REFINED MODEL OF THE 10S CONFORMATION OF SMOOTH MUSCLE MYOSIN BY CRYOEM 3-D IMAGE RECONSTRUCTION

Jun Liu, Dianne W. Taylor, Thomas Wendt and Kenneth A. Taylor
Institute of Molecular Biophysics, Florida State University,
Tallahassee, FL 32310

The actin-activated ATPase activity of smooth muscle myosin and HMM (smHMM) is regulated by phosphorylation of the regulatory light chain (RLC). Regulation requires two myosin heads because single-headed myosin subfragments are always active. 2-D crystalline arrays of the 10S form of intact myosin, which has a dephosphorylated RLC, were produced on a positively charged lipid monolayer. A homology model of smooth muscle myosin was constructed from the X-ray structures of the smooth muscle MDE and scallop muscle S1 structures and docked manually into the 2.0nm resolution cryoEM 3-D image. The initial models of both 10S myosin and smHMM were subjected to real space refinement to obtain a quantitative fit to the density. Both refined models reveal the same asymmetric interaction between the upper 50kDa domain of the "blocked" head and parts of the catalytic, converter domains and the essential light chain of the "free" head that were observed previously (Wendt et al. PNAS. 98, 4361(2001)). The 10S reconstruction shows considerably more S 2 than the smHMM reconstruction, but the location and direction of the initial segment of S2 is the same in both. This suggests that this part of the structure is not simply due to crystallographic packing but is enforced by elements of the myosin heads. Supported by NIH.

Poster 28

HOW WE CAN UNDERSTAND THE MECHANISM EXPRESSED BY THE ACTIN FILAMENT, BEING BASED ON THE ATOMIC STRUCTURE OF THE ACTIN FILAMENT COMPLEX

Yuichiro Maeda, Soichi Takeda, Atsuko Yamashita & Kayo Maeda; RIKEN Harima Institute at SPring-8, Kouto, Mikazuki, Hyogo, Japan 679-5148; ymaeda@spring8.or.jp

The actin filament plays a variety of important cellular functions throuth a variety of "molecular movement". Muscular contraction is driven by the sliding movement between myosin and the actin filament. In skeletal and cardiac muscles, the calcium regulation is likely to be performed through an allosteric transition of actin-tropomyosin-troponin complex. Recent studies have elucidated that polymerization-depolymerization of actin drives cellular locomotion as well as the organelle transportation.

The aim of our research work is to know the atomic structure of the actin filament (F-actin with/without actin associated proteins) which we believe to be indispensable information for understanding the mechanisms. This communication is a progress report of our recent studies.

One of our approach to this goal is to obtain the crystal structure of individual proteins separately. We previously solved the structure of a small complex of TnC with an N-terminal fragment of TnI (a.a. 1-47). We now have solved the crystal structure of troponin ternary complex (TnC, TnI and a C-terminal half of TnT, TnT1). Based on these structures, we now understand the mechanism how the calcium ion binding to TnC releaves the inhibitory action of TnI to actin-myosin interaction.

Our trials also include preparing a short and homogeneous segment of actin-tropomyosin (-troponin) complex which is suited for preparing crystals. As the first step for this strategy, we have solved crystal structures of tropomodulin (C-terminal half which interacts with actin) and CapZ ($\alpha\beta$-hetero dimmer), which should help us understanding how these proteins cap P- and B-ends of actin filament.

Poster 29

ATOMIC FORCE MICROSCOPY IN THE STUDY OF VIRUS PARTICLES, VIRUS CRYSTALS, AND VIRAL INFECTED CELLS

A. McPherson, Yu. G. Kuznetsov, A. J. Malkin, and M. Plomp; University of California, Dept. of Molecular Biology & Biochemistry, 560 SH, Irvine, 92697

Atomic Force Microscopy (AFM) is an effective technique for imaging virus particles within purified preparations, in crystalline form, and as they emerge from infected host cells. While the resolution of AFM does not approach that of X-ray crystallography, nor yet that of cryoelectron microscopy, it can, in many cases, resolve capsomeres and other structural features on virion surfaces. Its investigative range in three dimensions serves to bridge the size interval of 1 nm to 1 um lying between diffraction methods and light microscopy. We have used AFM to record a broad range of viruses ranging in diameter from 17 nm satellite plant viruses, to larger animal viruses such as herpes simplex (HSV) and mouse leukemic virus (MuLV) having diameters of about 100 nm, to even larger specimens such as irridoviruses and vaccinia. We present here images taken from a number of our investigations that include particles arrayed on mica substrates (tobacco mosaic virus (TMV), cauliflower mosaic virus (CaMV), tipula iridescence virus (TIV), and HSV), crystals of viruses ((turnip yellow mosaic virus (TYMV), satellite tobacco mosaic virus (STMV), and brome mosaic virus (BMV)), and budding virions (MuLV from infected NIH 3T3 cells). We have also used AFM to study the structural transformation in budding virions of the MuLV retrovirus that occurs as a result of genetic mutations, and to visualize the chemical and enzymatic dissection of HSV and vaccinia virus by detergents and proteases. From these latter studies, the architectural principles of very large viruses, which are not amenable to crystallography, and irregular or polymorphic viruses difficult to address with cryoelectron microscopy, can be structurally delineated. Our experiences have shown that established techniques used in electron microscopy, such as immunolabeling with gold particles, and traditional histological and chemical treatments used for tissues, cells, and macromolecules may be utilized as well with AFM and thereby broaden its applicability.

Poster 30

THREE-DIMENSIONAL STRUCTURES OF RNA POLYMERASE HOLOENZYME AND THE RNA POLYMERASE-PROMOTER OPEN COMPLEX: SYSTEMATIC FLUORESCENCE RESONANCE ENERGY TRANSFER AND DISTANCE-CONSTRAINED DOCKING

Vladimir Mekler, Ekaterine Kortkhonjia, Jayanta Mukhopadhyay, Achillefs N. Kapanidis, Andrei Revyakin, Yon W. Ebright, Jennifer L. Knight, Ronald M. Levy, and Richard H. Ebright; Howard Hughes Medical Institute, Waksman Institute, and Department of Chemistry and Chemical Biology, Rutgers University, Piscataway NJ 08854

We have used systematic fluorescence resonance energy transfer (FRET) and distance-constrained docking to define the three-dimensional structures of RNA polymerase holoenzyme and the RNA polymerase-promoter open complex in solution.

Our approach involves the following steps:

(i) incorporation of fluorescein at each of a series of sites within RNA polymerase core enzyme;

(ii) incorporation of Cy3 at each of a series of sites within s70;

(iii) incorporation of Cy5 at each of a series of sites within promoter DNA;

(iv)measurement of fluorescein-Cy3 and Cy3-Cy5 distances (>80 distances for RNA polymerase holoenzyme; >130 distances for RNA polymerase?promoter open complex); and

(v) distance-constrained structural docking of structures of RNA polymerase core enzyme, segments of s70, and segments of promoter DNA.

The resulting solution structures of RNA polymerase holoenzyme and the RNA polymerase-promoter open complex agree, in detail, with available crystallographic structures and define positions of segments of s70 not defined in available crystallographic structures.

Extensions of our approach permit monitoring of structural changes in RNA polymerase core enzyme, s70, and promoter DNA during transcription, permit measurement of kinetics of structural changes, and permit single-molecule measurement of the kinetics of structural transitions.

Poster 31

THE POLAR T1 INTERFACE IS LINKED TO CONFORMATIONAL CHANGES THAT OPEN THE VOLTAGE-GATED POTASSIUM CHANNEL

Daniel L. Minor, Jr. Department of Biochemistry and Biophysics, Cardiovascular Research Institute, University of California, San Francisco, CA 94131-0130

Kv voltage-gated potassium channels share an N-terminal cytoplasmic domain (T1) that forms tetramers and functions in channel assembly. Structure determination by X-ray crystallography of the T1 domain of the mammalian channel Kv1.2 together with alanine scanning mutagenesis and electrophysiological experiments identify clusters of residues on complementary surfaces of the unusual, buried, polar interface between T1 monomers that alter the voltage gating of the channel. Examination of an isosteric mutation in this interface that stabilizes the closed conformation of the channel, and increases the thermodynamic stability of T1 tetramers, shows little structural alteration as determined by crystallographic analysis. Replacement of T1 with sequences that form tetrameric coiled-coils supports channel assembly but destabilizes the closed conformation of the channel significantly. Together, these data suggest that T1 is a critical part of the gating machinery of Kv channels and that structural changes in the buried polar surface play a key role in the conformational changes that occur during channel gating.

Poster 32

MOLECULAR ARCHITECTURE OF THE PROTEIN IMPORT CHANNEL OF THE MITOCHONDRIAL OUTER MEMBRANE AND ITS LARGER MULTI-CHANNEL STRUCTURES

Kirstin Model[1], Thorsten Prinz[2], Teresa Ruiz[1], Michael Radermacher[1], Chris Meisinger[2], Nikolaus Pfanner[2] & Werner Kühlbrandt[1], [1]Max-Planck Institute of Biophysics, Department of Structural Biology, Heinrich-Hoffmann-Str. 7, 60528 Frankfurt, Germany; [2]Institute of Biochemistry and Molecular Biology, University of Freiburg, Hermann-Herder-Str. 7, 79104 Freiburg, Germany

To dissect the dynamic cooperativity of the outer mitochondrial translocation machinery in structural terms we analyzed the isolated TOM complex from the yeast Saccharomyces cerevisiae by single-particle electron microscopy. So far the major proportion of purified TOM complex of Neurospora crassa has revealed particles with two and three stain-filled pits resembling channels. However, on the molecular level the reason for that difference in the number of pores per complex has not been understood. By investigating the TOM complex from wild-type yeast and mutant yeast selectively lacking Tom20 we found in the first case three centers of stain accumulation whereas in absence of Tom20 two channel-like structures are found. This implies that Tom20 is involved in organizing Tom40 channels as basic translocation units into larger multi-channel structures.

Poster 33

MULTI-RESOLUTION CONTOUR-BASED FITTING OF MACROMOLECULAR STRUCTURES

Pablo Chacon Montes, Willy Wriggers; Department of Molecular Biology, TPC6, The Scripps Research Institute, 10550 North Torrey Pines Road, La Jolla, California 92037

New insights into cellular processes require the synthesis of information from low- to medium-resolution biophysical techniques, such as electron microscopy (EM), with atomic resolution structures. Here we present a novel approach for the registration of high-resolution structures with low-resolution densities that takes advantage of Fourier correlation theory to rapidly scan the translational and rotational pose of a probe molecule relative to a (fixed) target density map. The major advantage of this quantitative real-space docking method is that it enables multi-resolution surface matching using a Laplacian operator. Laplacian-filtered density maps maximize the fitting contrast: tests using synthetic low-resolution density models of single molecules indicate that the difference in score between the correct fit and spurious fits increases by 35-50% relative to correlation-based docking. The results also demonstrate the enhanced pose-recognition ability in the case of assemblies: it was possible to extend the resolution limit (to <30A) in witch can be unequivocally identify the correct docking pose. The algorithm will be applied to EM data sets from collaborating laboratories to demonstrate its practical effectiveness.

Poster 34

3D STRUCTURE OF THE CP43' PHOTOSYSTEM-I SUPER-COMPLEX OF CYANOBACTERIA REVEALED BY ELEC-TRON CRYO-MICROSCOPY AND SINGLE PARTICLE ANALYSIS.

Edward Morris, Thomas Bibby, Jonathan Nield and James Barber; Department of Biological Sciences Imperial College, London.

Certain cyanobacteria deficient in iron express the isiA gene coding for an intrinsic membrane protein known as CP43'. Recent electron microscope analysis [1,2] revealed that CP43' exists as part of photosystem-I supercomplex forming an 18 membered ring around the photosystem-I trimer. We have analysed the structure of the CP43' photosystem-I supercomplex by electron cryo-microscopy and single particle analysis obtaining a three-dimensional map at a resolution of ~25 Å. The density distribution within the photosystem-I domain allows accurate fitting of the 2.5 Å x-ray structure of the photosystem-I trimer [3], while the 18 CP43' domains in the outer ring match well with models of CP43' composed of 3 pairs of transmembrane helices. These observations allow us to build a detailed model of the complex and explore the mechanism by which light energy is transferred from the antenna ring to photosystem-I.

1. Bibby et al (2001) Nature 412 743.
2. Boekema et al (2001) Nature 412 745.
3. Jordan et al (2001) Nature 411 909.

Poster 35

STRUCTURAL BASIS OF TRANSCRIPTION INITIATION

K.S. Murakami, S. Masuda, E.A. Campbell, O. Muzzin, S.A. Darst, The Rockefeller University.

Promoter-specific transcription initiation by bacterial RNA polymerase (RNAP) requires the s subunit, which binds core enzyme ($\alpha_2\beta\beta'\omega$) to form holoenzyme. We crystallized *T. aquaticus (Taq)* holoenzyme with a 35 nt promoter DNA fragment. The crystals belong to space group $P4_322$, a = b = 182 Å, c = 524 Å, with one 453 kDa complex/AU. Diffraction is anisotropic, 4.5 Å x 7 Å. We solved the phase problem by MIR with heavy-metal clusters, using spherically averaged models for the structure of the clusters. Density modification gave an excellent 6.5 Å-resolution map (Fig. 1). We constructed a model of the holoenzyme/DNA complex by fitting the known structures of all the components - core enzyme (1), σ (2), and DNA - into the map and adjusting conformations (Fig. 1). We also solved *Taq* holoenzyme (4 Å resolution). The crystals belong to space group $P2_1$, a = 155.0 Å, b = 271.2 Å, c = 155.3 Å, β = 91.4°, with two 430 kDa molecules/AU. The structure was solved by a combination of molecular replacement, SIR with heavy-metal cluster, and density modification.

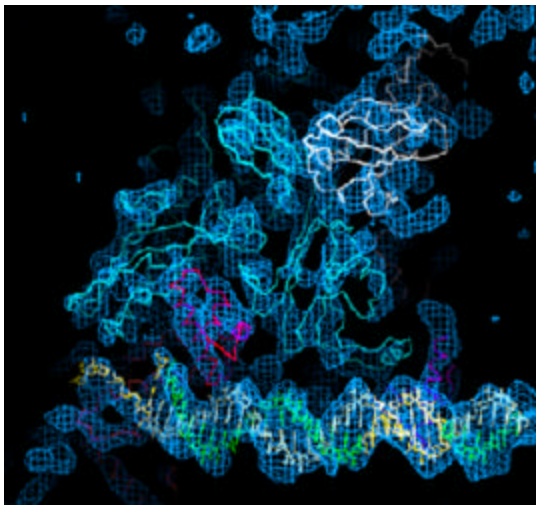

Fig. 1. 6.5 Å-resolution electron density map and model of the holoenzyme/DNA complex. RNAP α, white; β, cyan, σ, magenta. The DNA template strand is bright green, nontemplate strand is pale green, except the conserved promoter elements (yellow).

1) Zhang et al., Cell 98, 811.
2) Campbell et al., Mol. Cell, in press.

Poster 36

CONSISTENCY OF 3D RECONSTRUCTIONS IN SINGLE PARTICLE ANALYSIS

Pawel A. Penczek; Department of Biochemistry and Molecular Biology; University of Texas–Houston Medical School, 6431 Fannin, Houston, TX 77030, USA.

The consistency of 3D reconstructions is assessed with the help of resolution measures. The most commonly used measure, Fourier Shell Correlation (FSC), does not yield information about the three-dimensional (3D) distribution of variance in Fourier space; thus, it is of limited use in evaluation of 3D reconstruction validity. Therefore, we developed a 3D extension of the Spectral Signal-to-Noise Ratio (SSNR), which is defined as a ratio of the spectral power of the signal to the spectral variance. The 3D SSNR is derived for a class of 3D reconstruction algorithms that employ interpolation in Fourier space. The statistical properties of the SSNR are discussed and are related to the properties of FSC. The applicability of 3D SSNR ranges from the resolution estimation for 3D reconstructions with a very small number of available projections, such as tomography, to the resolution anisotropy evaluation for 3D reconstruction with highly uneven distribution of projections. Moreover, since 3D SSNR includes the spectral variance term, it becomes possible to evaluate the consistency of 3D reconstructions, particularly if the distribution of noise in input projections is known.

Poster 37

INTERACTION OF RELEASE FACTOR RF2 WITH THE RELEASE COMPLEX VISUALIZED BY CRYO-ELECTRON MICROSCOPY

Urmila B. Rawat[1], A. Zavialov[4], J. Sengupta[2], M. Valle[1], R.A. Grassucci[1], J. Linde[1], B. Vestergaard[5], M. Kjielgaard[5], M. Ehrenberg[4], and J. Frank[1-3]; [1]Howard Hughes Medical Institute, [2]Wadsworth Center and [3]Department of Biomedical Sciences, State University of New York at Albany, Empire State Plaza, Albany, New York 12201-0509, USA; [4]Department of Cell and Molecular Biology, BMC, Uppsala University, Box 596, 5-75124 Uppsala, Sweden; [5]Institute of Molecular and Structural Biology, University of Aarhus, Denmark.

Cryo-electron microscopy has been used previously to study the elongation cycle of protein synthesis (1). Here, a similar approach has been taken to explore the translational termination process, in the course of which a polypeptide is released from the ribosome by action of release factors RF1/RF2 and RF3 (2). As a first step in this investigation, various complexes were made between release complexes (2) and RF2(wt) or RF2 (Gly251Ala mutant) in the absence and presence of the antibiotic puromycin. This strategy is intended to explore the dynamic interaction of RF2 with the ribosome.

Three-dimensional cryo-EM maps were obtained for the complexes . The position of one of the domains of RF2 is found to overlap with the anticodon stem of the A-site tRNA. The recent X-ray structure of RF2 (3) has made it possible to describe putative sites of contact with the ribosome. Further work is in progress to obtain higher-resolution maps that allow insights into the interactions between the ribosomal machinery and the various domains of RF2.

The molecular mechanism by which the factor induces hydrolysis of the ester bond in the P-site peptidyl tRNA and the structural role played by the universally conserved GGQ region in RF2 will be investigated.

[Supported by NIH R37 GM29169, P41 RR01219, and NSF BIR 9219043 (to J.F.).]

References

1. R.K. Agrawal, C.M.T. Spahn, P. Penczek, R.A. Grassucci, K.H. Nierhaus, and J.Frank, J. J. Cell Biol. 79: 1670-1678 (2000).

2. A. Zavialov, R.H. Buckingham, and M. Ehrenberg, Cell, 107:115-124 (2001).

3. B. Vestergaard, L.B. Van, G.R. Anderson, J. Nyborg, R.H. Buckingham, R.H., and M. Kjeldgaard (submitted).

Poster 38

QUICK-FREEZE & FREEZE-SUBSTITUTION OF INSECT FLIGHT MUSCLE (IFM) FOR ELECTRON TOMOGRAPHY

M. K. Reedy[1], M. C. Reedy[1], C. Lucaveche[1], Y.E. Goldman[2], C. Franzini-Armstrong[2] & K.A. Taylor[3]; [1]Cell Biology, Duke Univ, Durham, NC; [2]Penn. Muscle Inst., Univ Penn, Philadelphia, PA; [3]Inst. Molec. Biophys., Fla State Univ, Tallahassee, FL

Permeabilized striated muscle is an ideal model for optimizing structural analysis of cellular machines, because preservation & resolution (even time-resolution) can be monitored by fiber X-ray diffraction while cryofixing/chemfixing & embedding for thin-section EM. Cryosectioning gives sections too thick, uneven & distorted to show myosin crossbridge forms and extended lattice order. But flat, uniform 25 nm sections are easily cut from Araldite-embedded insect flight muscle after quick-freeze freeze-substitution, so we will push this to its resolution limit. Fixed-embedded fibers diffract to 1.6 nm (native patterns to =1.3 nm), but EMs cut off at ~5 nm, a puzzle. Limits include 7Å Araldite "texture", and nano-granularity of section-stains (U, Pb, Mn, etc.) as they permeate embedded microstructures, "decorate" proteins and coarsen in the beam. But recall that post-embedding immuno-EM proves preservation of complex epitope structures. Quick-freeze vitrification, then freeze-substitution (solvation of ice) in acetone at -80°-93° C should allow chemical cross-linking of native structure stabilized well below the critical -60° C that arrests sidechain mobility (G. Petsko). Promising options to be tried include cryodiffraction of quick-frozen fibers (70 µm x 6 mm) during freeze-substitution, and cryo-embedding in UV-catalyzed resins.

IFM fibers can vitrify to 5-8 µm depth w/o cryoprotectant (CP) when slam-frozen on LHe_2-cooled metal, but if plunge-frozen at -196° C need 15% glucose (best!) to vitrify, slower but deeper. Impact-shock perturbations are usual in slam-frozen lattices, unusual in plunge-frozen. Plunging in a spinning pot of LN_2-slush at -209° C should freeze faster than ethane-propane at -196°C. Freeze-substitution by cryo-TAURAC (tannic acid, then uranyl acetate, in -80°C acetone) gives superior preservation. But a dense 1 nm surface coating of myofilaments by TA-metal often complicates 3D imagery, calls for cryo-solvent tweaking to promote uniform stain permeation. (Supp by NIH-NIAMS, NIGMS).

Poster 39

A METHOD FOR CREATING A HIGH-RESOLUTION PROJECTION DIFFERENCE MAP

Gang Ren, Alok K. Mitra; Department of Cell Biology, The Scripps Research Institute, MB21, La Jolla, CA 92037

Completely side view of protein had had to be collected for single particle analysis on cryo-electron microscope. However, it is difficult to tilt a protein in thin layer of buffer, especially to the proteins with hydrophobic surface, flat proteins and ring-like protein. Protective antigen fragment of Anthrax toxin, PA63, explores a large hydrophobic surface when a N-terminal fragment is released by the cell-surface protease furin[1]. This surface causes the whole protein float on both surfaces of thin buffer layer on a holly grid before frozen. This means that only images closed to "top/bottom" of view of particles can be collected on EM. Artificially, to homogenize the surface, by incubated with same detergents or lipids, may cause losing of binding ability to Anthrax Lethal Factor (LF) on this hydrophobic surface. Therefore, only difference project map can be investigated on LF binding to PA63. In the images analysis, ignoring small titled angle of particles is fatal. For instant, as a 400kDa protein with100Å thickness, the projections of top and bottom molecular can be shifted to 30Å due to ± 8° tilt on this molecular. Utilizing EMAN program packages[2], a protocol to refine high-resolution projection map in considering of small tilt angle of particles is introduced. Moreover a program of centralizing and orientalizing projection maps is developed for creating a projection difference map of different weighted molecules, e.g. PA63 and its LF complex. A dissolved LF bind to PA63 heptamer center domain is discovered based on the difference map.

Reference: 1. Petosa, C., etc., Crystal Structure of the anthrax toxin protective antigen, Nature, 385(1997), 833-838. 2. Ludtke, S., etc., EMAN: Semiautomated Software for high-Resolution Single-Particle Reconstructions, J. Struct. Biol., 128(1999), 82-97

Poster 40

CRYSTALLOGRAPHIC ANALYSIS OF A 3.6 MILLION DALTON RESPIRATORY PROTEIN

W.E. Royer & K. Strand, University of Massachusetts Medical School, Worcester, MA

Many annelids, including the earthworm, Lumbricus terrestris, have giant cooperative respiratory proteins freely dissolved in the blood. These complexes, termed either erythrocruorins or hemoglobins, are assembled from many copies of both hemoglobin subunits and non-hemoglobin or "linker" subunits. The crystal structure of Lumbricus erythrocruorin was determined using models based on cryo EM images to phase the diffraction data to 26 Å resolution followed by molecular averaging to extend the phasing to 5.5 Å resolution (1). This structure reveals a remarkable hierarchical organization of 144 oxygen binding hemoglobin subunits and 36 linker subunits assembled into a complex with D6 symmetry. The fundamental molecular unit, one-twelfth of the whole molecule, comprises a dodecamer of hemoglobin subunits and a mushroom-shaped trimeric linker complex. Each linker trimer projects a triple-stranded coiled-coil "spoke" whose interdigitation with neighboring spokes appears crucial for stabilization. This structure is being extended to 3.5 Å and will be combined with crystallographic analysis of an isolated hemoglobin dodecamer and structural analysis of the deoxygenated molecule to decipher the structural basis for assembly and cooperativity.

1) Royer, W.E., Strand, K., van Heel, M. and Hendrickson, W.A. (2000) Proc. Natl. Acad. Sci. 97, 7107-7111

Poster 41

RECONSTRUCTING HELICAL OBJECTS USING SINGLE PARTICLE IMAGE PROCESSING, MULTIVARIATE STATISTICAL ANALYSIS, AND A TOMOGRAPHIC RECONSTRUCTION ALGORITHM

Rasmus R. Schroeder, Isabel Angert, Joachim Frank*, Kenneth C. Holmes; Max-Planck Institute for medical research, Biophysics Dept., Heidelberg, Germany; *Howard Hughes Institute, Wadsworth Center, Albany, USA

Helical objects can be thought of as 1D crystals. The original Fourier-Bessel reconstruction algorithms take advantage of this. However, such methods do not take account of disorder along the helix axis and consequently their application reduces the attainable resolution. Recent work has used conventional single particle image processing techniques applied to short lengths to overcome this lack of order. Applying such procedures to myosin-S1-decorated actin filaments does in fact lead to some increase in resolution. However, analysis of the data shows there is a residual uncertainty in the projection angle f orthogonal to the filament axis that still limits resolution. Although changes in f significantly affect the appearance of 2D projections they cannot be quantified by standard 2D alignment methods such as cross-correlation functions. However, the use of Multivariate Statistical-Analysis (MSA) to classify projections of the initial low resolution model at known projection angles f leads to a specific 1D curve in factor space. After correcting signal strength, resolution and CTF the original experimental images can directly be mapped onto this 1D hyper space, thus determining the projection angle f. The known projection geometry is then used to define an inverse axial tomography problem, which is solved by least-squares methods.

Poster 42

THE QUATERNARY STRUCTURE OF NITRILASES FROM 2NM NEGATIVE STAIN MAPS AND HOMOLOGY MODELLING

B.T. Sewell and MN Berman; University of Cape Town, South Africa

The nitrilases are members of a widespread superfamily of enzymes that cleave non-peptide C-N bonds. They have been exploited industrially - most notably in the production of acrylamide and are of interest in the detoxification of cyanide waste. The crystal structures of two members of the superfamily, Nit and DCase, are known.We have obtained 2nm resolution single particle reconstructions of two cyanide dihydratases from *Bacillus pumilus* and *Pseudomonas stutzeri*. The enzymes have 70% sequence homology to one another and have a subunit molecular weight of 37kDa. The enzymes are typical of their class in that they exist as large complexes having molecular weights greater than 500kDa and they differ from the two enzymes of known atomic structure which form tetramers with 222 symmetry.

The three dimensional maps reveal that the quaternary complexes are defined length, strained, right-handed helices with a global dyad axis, comprising 14 subunits in the case of the *P. stutzeri* enzyme and 18 subunits in the case of the *B. pumilus* enzyme. Structural homology with Nit and DCase which have less than 20% sequence homology enables the construction of plausible models of the cyanide dihydratases. The cyanide dihydratases have three deletions of 5-8 amino acids and two insertions of 13 and 14 amino acids all of which occur in externally located loops, and a substantial C-terminal extension of 30-40 amino acids. If it is assumed that the one of the dimer axes present in Nit and DCase is preserved in the helix then the

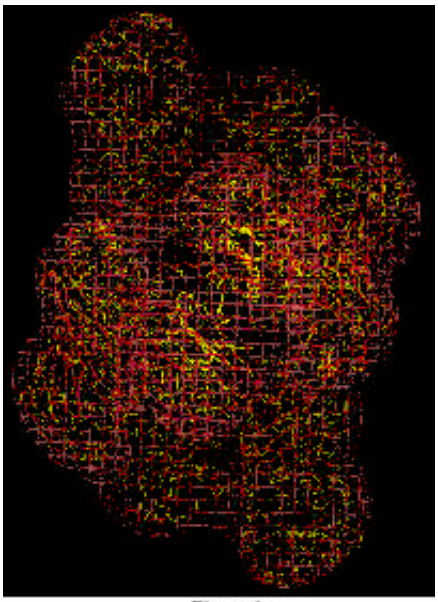

Figure 1

dimer model can be positioned with precision. The observed density is consistent with only one of the four possible placements. Measurements made from a cylindrical projection of the density enabled the other dimers to be placed by application of the appropriate rotations and translations. The details of the fit were then refined manually using O (Figure 1).

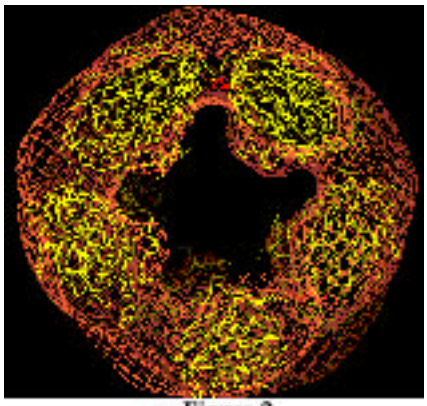

Figure 2

The model enables the identification of the regions of inter-subunit contact to be identified as well as the extent and nature of the strain accumulation in the helix. Intersubunit contacts not found in Nit and DCase occur in regions near the insertions, one of the deletions and the C-terminal extension. Helix formation is enabled by the formation of a contact involving the C-terminal extension the space for which can be seen in figure 2. The irregular helix suggests that interaction involving the C-terminal extension is not rigid and this in turn suggests a reason for the short length of the helix. It grows by addition of dimers until distortions mount up to the extent that steric hindrance prevents the addition of a further dimer.

Poster 43

THE STRUCTURE OF THE EUKARYOTIC 80S RIBOSOME FROM *S. cerevisiae*

Christian M.T. Spahn[1, 2], Roland Beckmann[4, 5], Narayanan Eswar[7], Pawel A. Penczek[6], Andrej Sali[7], Günter Blobel[4] and Joachim Frank[1, 2, 3]; [1]HHMI, Health Research Inc. at the; [2] Wadsworth Center, Empire State Plaza, Albany, NY; [3]Department of Biomedical Science, SUNY at Albany; [4]Laboratory of Cell Biology, HHMI, The Rockefeller University, New York, NY; [5]Institut für Biochemie der Charité, Humboldt Universität zu Berlin, Germany; [6] University of Texas - Houston Medical School, TX; [7]Laboratory of Molecular Biophysics, The Rockefeller University, New York, NY

A cryo-EM reconstruction of the yeast 80S ribosomes was computationally separated into rRNA and protein densities and further analyzed by docking models for the rRNA and homology models of yeast ribosomal proteins. This analysis presents an exhaustive inventory of an eukaryotic ribosome at the molecular level. Strikingly, the core of both subunits shows a remarkable conservation among species from different kingdoms. However, some significant differences in functionally important regions and dramatic changes in the periphery are evident. Furthermore, the molecular components involved in subunit interaction are highly conserved, with the exception of four new contact points at the periphery. Our model of the yeast 80S ribosome provides the basis for molecular-level interpretations of the interactions of the eukaryotic ribosomes with its ligands such as tRNAs, EF-2 (1) and the HCV IRES RNA (2).

(1) Gomez-Lorenzo et al., (2000) EMBO J. 19: 2710-2718
(2) Spahn et al., (2001) Science 291: 1959-1962

Poster 44

EM ANALYSIS OF LARGE, MULTI-SUBUNIT TRANSCRIPTIONAL REGULATORY COMPLEXES REVEALS DISTINCT, ACTIVATOR-DEPENDENT CONFORMATIONS

Dylan J. Taatjes[1], Anders M. Näär[2], Eva Nogales[1], and Robert Tjian[1]; [1]Howard Hughes Medical Institute, Department of Molecular and Cell Biology University of California, Berkeley.; [2]Department of Cell Biology, Harvard Medical School Massachusetts General Hospital Cancer Center.

The related human coactivators ARC-L and CRSP (approximately 2.0 and 1.2 MDa in size) are part of a family of multi-subunit cofactor complexes that are generally required for transcription and are targeted by a diverse array of regulatory proteins (nuclear receptors, p53, NF-κB, SREBP, VP16, and others). However, only CRSP potentiates activator-dependent transcription in vitro. To gain insight into their mechanism of action, we conducted structural and functional analyses of the ARC-L and CRSP cofactors. Structural studies utilized electron microscopy and single-particle image reconstruction techniques with negatively-stained samples. EM analysis of CRSP reveals that this large complex is capable of adopting multiple stable conformations. Further, these conformations appear to be activator-specific and induced upon activator binding. The structures (reconstructed to 32 Å or better) of unliganded CRSP or CRSP bound to VP16 or SREBP revealed dramatic structural differences. These differences were further substantiated by a series of experiments that converted unliganded (activator-free) CRSP selectively and specifically to its distinct activator-bound conformations. Conformational changes were verified by EM analysis and cross-correlation of the structures. Additional antibody-labeling experiments mapped the VP16 and SREBP binding sites to comparatively small and discrete regions on the CRSP complex. Mechanistic implications of these findings will be discussed.

Poster 45

IMAGE RECONSTRUCTION FROM CRYO-ELECTRON MICROGRAPHS OF IN VITRO ASSEMBLED TUBES OF HIV-1 P24 CAPSID AND CAPSID-NUCLEOCAPSID PROTEIN REVEALS POTENTIAL SUBUNIT INTERACTIONS INVOLVED IN ASSEMBLY

Dennis R. Thomas*, Jason Lanman*, Thomas Wilk#, Stephen Fuller# and Peter E. Prevelige*. *Dept. of Microbiology, University of Alabama Birmingham, #Division of Structural Biology, Welcome Trust Center for Human Genetics,Unversity of Oxford, Oxford, England.

Purified recombinant HIV-1 capsid and capsid-nucleocapsid proteins can be assembled in vitro, forming cones, tubes or spheres in a manner dependent on assembly conditions and the exact construct assembled. Each of these forms have characteristics similar to either the immature particle or mature capsid of HIV. These in vitro assembled complexes are good candidates for structural studies by EM.

Reconstructions will be presented from electron micrographs of in vitro assembled tubes of both p24 capsid (CA) and the capsid-nucleocapsid (CANC) proteins. All reconstructions reveal a P6 like lattice of hexamers covering the surface of the tube. Adjacent hexamers are connected by density lying at lower radius between hexamers. The density of the outer surface hexamers can be fit with the known structures (x-ray and NMR) of the N-terminal domain. The C-terminal domain x-ray structures can be fit into the density connecting the hexamers in our maps. The models built into the CANC reconstructions reveal subunit interfaces, which may mediate assembly.

The capsid protein forms a dimer by association of two C-terminal domains. No higher order oligomer has ever been observed to form between N-terminal domains even though they are clearly associated in the EM reconstructions. Based on this model, we are making specific mutations, which we believe will affect the assembly of the capsid protein. It is hoped that a higher order N-terminal intermediate can be stabilized and identified. The various wild type and mutant capsid proteins will be characterized *in vitro* by monitoring the kinetics of assembly, varying protein concentration, ionic strength and pH. The mutations examined to date have shown both large increases and decreases in the rate of assembly, relative to wild type. Changes in the critical concentration of protein

required for assembly correlate with changes in rate of assembly. One example, the mutation of a histidine at residue 12 to either, alanine, lysine or glutamate shows distinctly different behaviors. Alanine exhibits nearly wild type properties, substitution with glutamate reduces the rate of assembly and increases the critical concentration and the substitution with lysine results in a > 10 fold increase in rate of assembly. The products of these *in vitro* assembly reactions are being examined by electron microscopy.

H/D mass spectrometry of capsid protein assembled *in vitro* is also being used to identify regions of the protein, which become protected or more exposed as a consequence of assembly. Regions of the capsid protein, particularly helices 3 and 4, have been identified which exhibit 1000 fold increases in protection from deuterium exchange upon assembly. The pattern of protection can be used to assess the validity of the atomic model fit to the reconstructions and identify sites important for assembly.

Mutations, which appear to stabilize the capsid *in vivo* are less infectious than wild type. These same mutations also show increased rates of assembly in vitro. Using the available mutational data, combined with these structural, biochemical and biophysical techniques we hope to identify intermediates in the assembly pathway, which have to date proven elusive.

Poster 46

3D MOTIFS: STRUCTURE & FUNCTION PREDICTION

Jerry Tsai, Texas A&M University, Department of Biochemistry & Biophysics

The rapid increase in genomic information demands more automatic methods for protein function and structure determination. Such methods will become fundamental tools that make the enormous amount of sequence data accessible to researchers in the health sciences. A computational approach to protein function and structure prediction has been chosen. In an informatics study focused on understanding protein tertiary contacts, the protein structure database will be mined for non-local interactions between recurrent local, secondary structure elements. From this analysis, a database will be constructed of tertirary contacts between repetitive, local structure pairs: the 3D Motifs library. As the first step, a list of interacting, secondary structure pairs will be generated based on four non-local interactions: disulfide bonds, salt bridges, hydrogen bonds, and hydrophobic contacts. The resulting fragment pair list will be clustered to find the repetitive secondary structure pairs or 3D Motifs. Sequence and structural information will be extracted in an analysis of each cluster each motif will be organized into a searchable and browsable database (the 3D Motifs library). The 3D Motifs library will lend itself well to both function and structure prediction. For function prediction, an initial characterization of known functions from sequence and structural alignments will be made to identify only those residues important for a protein's function (functional signature). Additional analysis using the 3D Motifs library will expands out the identification of function from residues to secondary structure. Now, the prediction of function will no longer be tied to the linear sequence or structure, but now focuses on a group of interacting secondary structure elements. For structure prediction, the 3D Motifs will be used to identify non-local contacts. These will be used to generate starting conformations before structure generation; to constrain the structure during generation; and to post-filter after structure generation. In effect, the method will reduce conformational search space and increase the probability of generating native-like folds. This general survey and classification of tertiary interactions will help in making the overwhelming amounts of genome information more approachable.

Poster 47

AN ALL-ATOM HOMOLOGY MODEL OF THE *E. COLI* 30S RIBOSOMAL SUBUNIT

C.-S. Tung, Los Alamos National Laboratory, K. Sanbonmatsu, Los Alamos National Laboratory, S. Joseph, UCSD

Ribosome is the molecular entity that translates genetic codes into proteins. Its detailed structure is the information necessary for understanding the translational step of the protein biosynthesis. The solving of the *Thermus thermophilus* 30S ribosomal subunit crystal structure(1FJF in PDB) makes it possible to predict structures of 30S ribosomal subunits from other organisms. Here, we describe the modeling of the *Escherichia coli* 30S ribosomal subunit using a homology modeling approach. The template (*T. thermophilus*) and the target (*E. coli*) 16S RNAs are having an overall 76% sequence identity. The highly homologous sequences as well as the similar secondary structural folds make it a good candidate for predicting the *E. coli* 16S RNA structure using a homology modeling approach. We have developed a homology modeling algorithm utilizing a motif modeling protocol for predicting the *E. coli* 16S RNA structure. The sequences of the target and the template ribosomal proteins (S2 to S20) are highly homologous with sequence identities range from 35% to 75%. These ribosomal protein structures were also constructed using a homology modeling approach. The resulting structure of the E. coli 30S ribosomal subunit is subjected to energy minimization using AMBER. The energy minimized model structure (shown in yellow) compared favorably with experimental observation (shown in black) as depicted in the figure. The cryo-EM data used for comparison in this figure was kindly supplied to us by Prof. Joachim Frank of SUNY Albany.

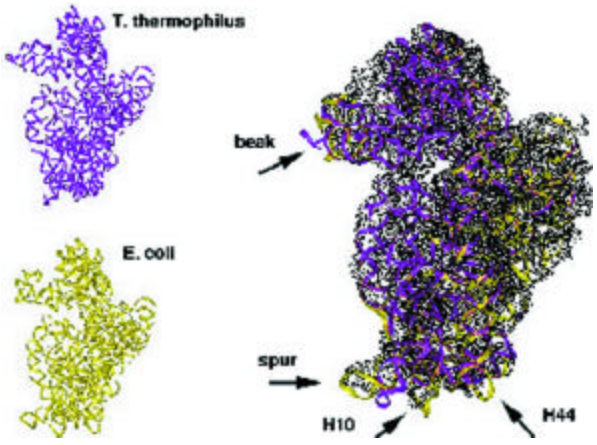

Poster 48

INTERACTION OF EF-G WITH POST-TERMINATION RIBOSOMES STUDIED BY CRYO-ELECTRON MICROSCOPY.

M. Valle[1], A. Zavialov[2], J. Sengupta[3], U. Rawat[1], M. Ehrenberg[2] & J. Frank[1]; [1]Howard Hughes Medical Institute, Heath Research, Inc., [3]Wadsworth Center, Empire State Plaza, Albany, New York 12201-0509, USA; [2]Department of Cell and Molecular Biology. Biomedical Center, S-75124 Uppsala, Sweden.

During the last years cryo-EM has been employed to depict the ribosome in different steps of protein biosynthesis. The technique has revealed the way some factors bind to the ribosome; the positions of tRNAs; the pathways for the mRNA and for the synthesized polypeptide; and conformational changes within the ribosome. In the case of Elongation Factor G (EF-G) there are several previous structural data based on cryo-EM maps1 that represent ribosome-bound complexes. The GTPase activity of the factor drives the movement of the tRNAs and the translocation of the mRNA by one codon, while EF-G binding alone changes the relative positions of the ribosomal subunits. Here we present cryo-EM three-dimensional reconstructions of several complexes formed between post-termination E.coli ribosomes2 and EF-G. A high resolution map of a puromycin-treated post-termination ribosome complex with EF-G and a GTP analog allows us best to characterize the interaction of the factor with the ribosome. The map shows that the P-site deacylated tRNA has been translocated as in the elongation cycle, but its position is a clear hybrid between the previously-described P and E sites.

[Supported by NIH R37 GM29169, P41 RR01219, and NSF BIR 9219043 (to J.F.)]

1. R. Agrawal, P. Penczek, R. Grassucci & J. Frank. Proc. Natl. Acad. Sci. USA 95: 6134-6138 (1998).
2. A. Zavialov, R. Buckingham, and M. Ehrenberg. Cell 107: 115-124 (2001).

Poster 49

ANALYSIS OF HETEROGENEOUS COMPLEXES BY COMBINED STATISTICAL ANALYSIS AND REFERENCE MATCHING

H. White[1], Shaoxia Chen[1,2], Brent Gowen[3], Johannes Buchner[4] , H. Saibil[1], E. Orlova[1]; [1]School of Crystallography, Birkbeck College, London, UK, [2]Dept of Bioscience, Imperial College, London, UK, [3]Wellcome Trust Centre for Human Genetics, Oxford, UK, [4]Institut für Organische Chemie und Biochemie, Technische Universität, München, Garching, Germany

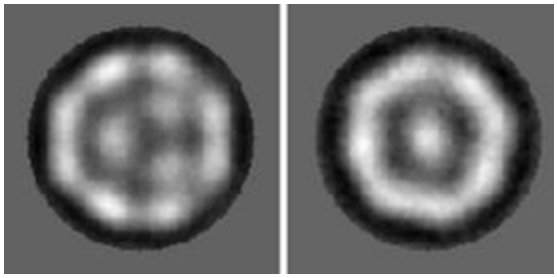

Fig.1

When imaging a population of biologically active complexes it is not always possible to trap all the molecules in solution in the same state. In our analysis of the yeast small heat shock protein Hsp26, we find complexes of 24 subunits of 26 kDa each(1). Although the particles all have tetrahedral symmetry and are biochemically homogeneous, the image data set is not consistent with a single structure.

Multivariate statistical analysis (2) clearly revealed the presence of particles with different sizes, demonstrated by the eigenimages. A data set of ~15, 000 particles was sorted into five groups. The largest group (~9200 images) contained large diameter particles, and another class contained ~2900 small particles. The remaining groups presented a population of mixed size particles. Fig.1 shows sums of the large (left side, 190 Å diameter) and small particles (right image, 180 Å).

Classification has revealed images of particles with different structural features (Fig 2). These classes have been used to calculate

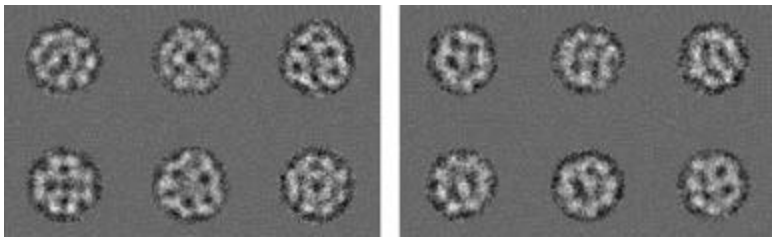

Fig.2 Large particles Small particles

3D reconstructions and projections of the models have been used to refine separation of images into two groups.

For this step, we used the projection matching approach (3). Eventually we were able to obtain reconstruction of the two forms, showing similar assemblies but different packing of domains inside the shell-like structures.

1. Haslbeck M., Walke S., Stromer T., Ehrnsperger M., White HE., Chen S., Saibil HR., Buchner J. (1999) Hsp26: a temperature-regulated chaperone. EMBO J. 18, 6744-6751.
2. Van Heel M., (1987), Classification of very large electron microscopical image data sets. Optic. 82, 114-126
3. Penczek P., Grassucci R., and Frank J., (1994), The ribosome at improved resolution: new techniques for merging and orientation refinement in 3D cryoelectron microscopy of biological particles. Ultramicroscopy, 53, 251-270

Poster 50

STRESS-INDUCED PROTEIN/DNA CRYSTALLINE ARRAYS OBSERVED IN-SITU BY ELECTRON TOMOGRAPHY

Sharon Grayer Wolf*, Daphna Frenkiel-Krispin#, Eyal Shimoni* and Abraham Minsky#; *Electron Microscopy Center, #Organic Chemistry Department, Weizmann Institute of Science, Rehovot 76100 ISRAEL

Ordered systems and processes in living organisms are usually energy-dependent. Examples of these are the translocation of motor proteins across their substrates, and the energy-driven polarized conformational changes exhibited by multiple-component macromolecules like ribosomes, spliceosomes and proteasomes. In particular, DNA-repar processes are strictly depend upon energy consumption. But when stressed by starvation or harsh environments that lead to energy depletion, bacteria have evolved a protection strategy, whereby order in the cell switches to passive mode by inducing DNA/Dps crystals in-vivo. Upon reintroduction of nutrients, the crystals disappear and normal functioning resumes in the cell. By this sequestration, the DNA is protected passively from damaging agents. We will present a tomographic study by Electron Microscopy, of such crystalline systems from flash-frozen, freeze-substituted sections of starving bacteria.

Poster 51

A METHOD TO STUDY THE STRUCTURE OF FUNCTIONAL CHANNELS AND TRANSPORTERS IN THEIR NATIVE ENVIRONMENT.

G.A. Zampighi[1-2], S. Lanzavecchia[3], M. Kreman[1], L. Zampighi[2], E. Turk[2] and E. Wright[2]. Departments of Neurobiology[1] and Physiology[2], UCLA School of Medicine. Dipartimento di Chimica Strutturale[3], Universita di Milano.

The elucidation of the structure of "functional" channels and transporters has progressed slowly because of difficulties with purification and crystallization. In addition, their molecular weights are often below the resolution of the single particle cryo-electron microscopy technique (~500 kDa). To collect structural information of functional channels and transporters in their native environment, we optimized the shadowing method and produced thin homogeneous metal layers representing faithful replicas of the outer shell of the channels. The replicas were imaged using random conical tilt conditions (i.e., the same particle was imaged un-tilted and tilted 50°). We studied the structure of purified aquaporin-0 (AQP0), a tetramer ~114 kDa molecular weight that functions as a water channel in lens fiber cells. First, we collected several data sets to optimize the experimental conditions and selected a data set of 2,547 particle pairs for analysis. The un-tilted images were classified using multi-reference analysis and partitioned into classes representing the cytoplasmic and external surfaces of the channel. The tilted images were used to calculate the three-dimensional models of the metal replica representing the surface of the channel (the "mould"). The inner surface of the mould was used to calculate the "imprint" that represented the shell structure of the exposed surfaces of the channel. Up to 2 nm resolution, the three-dimensional model of the outer shell appeared very similar to that predicted for the glycerol-conducting channel using x-ray diffraction methods.

Poster 52

STRUCTURE OF DENGUE VIRUS: IMPLICATIONS FOR FLAVIVIRUS ORGANIZATION, MATURATION, AND FUSION

Wei Zhang*, Richard J. Kuhn*, Michael G. Rossmann*, Sergei V. Pletnev*, Jeroen Corver#, Edith Lenches#, Christopher T. Jones*, Suchetana Mukhopadhyay*, Paul R. Chipman*, Ellen G. Strauss#, Timothy S. Baker*, & James H. Strauss#; *Department of Biological Sciences, Purdue University, West Lafayette, IN 47907-1392, USA. # Division of Biology 156-29, California Institute of Technology, Pasadena, CA 91125, USA.

The first structure of a flavivirus and its immature form have been determined by using a combination of cryo-electron microscopy and fitting of the known structure of glycoprotein E into the electron density map. Both reconstructions demonstrate densities of the capsid core, the lipid bilayer, and the external, icosahedral scaffold of 180 copies of glycoprotein E. The mature virus consists of 90 glycoprotein E dimers, whereas the immature form of the virus, which contains the precursor membrane protein (prM), has 60 glycoprotein E trimers. Cleavage of prM by the cellular protease furin induces the re-organization of glycoproein E, and activates the flavivirus particles for fusion during virus entry. The structure suggests that flaviviruses, and by analogy also alphaviruses, employ a fusion mechanism in which the distal beta-barrels of domain II of the glycoprotein E are inserted into the cellular membrane.

Poster 53

IMIRS: A HIGH-RESOLUTION 3D RECONSTRUCTION PACKAGE INTEGRATED WITH A RELATIONAL IMAGE DATABASE

Z. Hong Zhou, Eugene Y. Ke, Yuyao Liang; Department of Pathology and Laboratory Medicine, University of Texas - Houston Medical School, Houston, TX 77030, USA

The development of computer-controlled electron microscopes equipped with higher voltage, more coherent field emission electron sources, and better specimen stages has made it possible to image macromolecular machines to near atomic resolution by electron cryomicroscopy (cryoEM). However, both empirical experience in improving the resolution in cryoEM reconstructions [1-4] and theoretical estimation based on comparisons of the scattering power of electrons and x-ray photons of biological samples[5] have suggested that the number of particle images required increases exponentially as the targeted resolution of the three-dimensional (3D) structure improves. It has become clear that further progress towards higher resolution requires a consistent effort not only to improve existing image processing methods, but also to introduce better means of data management.

In an effort to improve the throughput of high-resolution 3D structure determination of macromolecular complexes, we have developed a distributed relational database of structured query language (SQL) for managing the complex datasets and integrated it into our high-resolution Image Management and Icosahedral Reconstruction System (IMIRS). IMIRS consists of a complete set of modular programs for icosahedral reconstruction organized under a graphical user interface (GUI) and provides options for user-friendly, step-by-step data processing as well as automatic reconstruction (Fig. 1 a-c). In IMIRS, the conventionally unorganized intermediate parameters and processing information are seamlessly managed by a database, relieving users from the tedious data management and allowing them to focus on processing tasks. The integration of data management with processing in IMIRS automates the tedious tasks of data management, enables data coherence, and facilitates information sharing in a distributed computer and user environment without significantly increasing the time of program execution. Several examples will be presented to illustrate the applicability of IMIRS in image management, image assessment (such as molecular size differences of the pyruvate dehy-

drogenase complexes), and high-resolution reconstructions of several medium to large size viruses (Fig. 1c-f).

Acknowledgement: This research is supported in part by NIH (AI46420), the Welch Foundation (AU-1492) and the March of Dimes Foundation (5-FY99-852). We thank Dr. W. Chiu for encouragement, Prof. J.-Q. Zhang at Zhongshan University, China for providing the CPV sample and J. Jakana for the cryoEM images used in Figure 1.

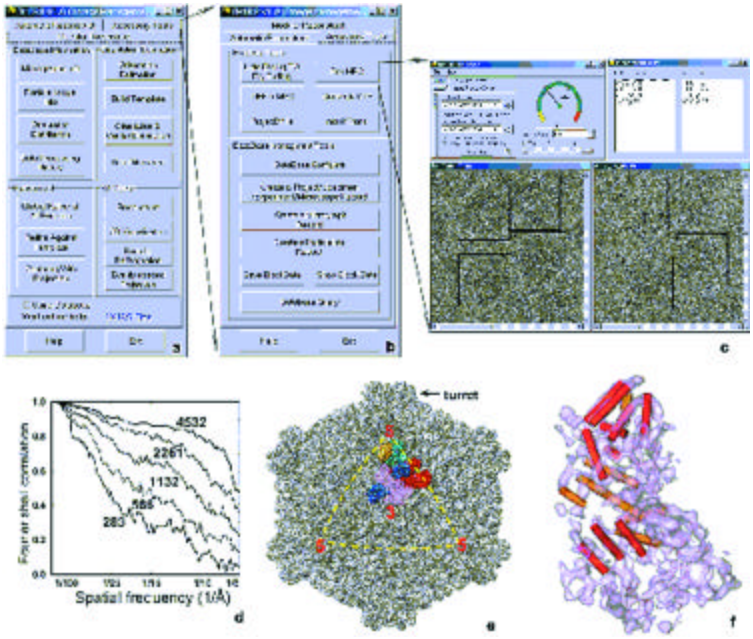

Figure 1. (a-c) Graphical user interface (GUI) showing the modular programs and data management tools in IMIRS. (a) IMIRS GUI consists of three program tabs. The programs in the *Modular Reconstruct* tab are arranged into four distinctive categories: *Database Information* (modules for image database query), *Orientation Estimation* (modules for estimating particle orientation and center, as well as size difference evaluation), *Refinement* (modules for global and projection-based refinement of orientation and center parameters), and *3D Model* (modules for reconstruction, visualization, and re-projection). (b) *Accessory Tools* tab contains modules for format changes, image manipulation, database configuration and management tools. (c) *BoxMRC*: a program available in the *Accessory Tools* tab for "boxing" out particles interactively from far-from-focus micrograph (left) and for automatic particle match-

ing in the close-to-focus micrograph (right) of a focal pair. (d-f) Application of IMIRS programs in the 3D reconstruction of the cytoplasmic polyhedrosis virus (CPV). (d) Fourier shell correlation coefficient as a function of spatial frequency between independent reconstructions calculated from the two halves of each data set of different number of particles (indicated near each curve). (e) Shaded surface view of the 8-Å reconstruction of CPV viewed along a 3-fold axis. One icosahedral face is outlined by the dashed lines with icosahedral 5- and 3-fold axes labeled. (f) Helices (shown as cylinders of 5 Å in diameter) identified are superimposed on the semi-transparent densities of a monomer of the capsid shell protein.

References:

1. Mancini, E. J., Clarke, M., Gowen, B. E., Rutten, T. & Fuller, S. D. Mol Cell 5, 255-66 (2000).
2. Böttcher, B., Wynne, S. A. & Crowther, R. A. Nature 386, 88-91 (1997).
3. Conway, J. F. et al. Nature 386, 91-4 (1997).
4. Zhou, Z. H. et al. Science 288, 877-80. (2000).
5. Henderson, R. Quart Rev Biophys 28, 171-193 (1995).

Poster 54

THREE-DIMENSIONAL ORGANIZATION OF THE HUMAN PLATELET INTEGRIN $a_{IIb}b_3$

Brian D. Adair and Mark Yeager, The Scripps Research Institute

Integrins are a family of heterodimeric, transmembrane signaling proteins theat affect diverse biological processes. We have used electron cryo-microscopy and threee-dimansional image reconstruction to examine the structure of the unliganded (low affinity) state of the human platelet integrin $\alpha_{IIb}\beta_3$ Mature, glycosylated $\alpha_{IIb}\beta_3$ was isolated from outdated human platelets solublized in β-octylglucoside using cell fractionation techniques and purified with ion exchange and gel filtration chromatography. Images of frozen-hydrated particles were processed using EMAN software, and a map at 20 Å resolution was derived from 3,108 particles. The large extracellular domain is comprised of a head and body. The long axis of the body is rotated ~ 60° with respect to the long axis of the head. This contrasts with the ~ 130° angle between the head and body in the crystal structure of the αVβ3 ectodomain, which may be due to conformational changes arising from the different activation states of the two integrins. A rod of density that we interpret as two parallel α-helices connects the large ectodomain and small cytoplasmic domain. Arguments based on conservation of residues at the protein-protein interface predict that the a-helices pack as a right-handed coiled-coil.

Poster 55

CRYSTAL STRUCTURE OF THE UPPER DOMAIN OF VP5, THE MAJOR NUCLEOCAPSID PROTEIN OF HERPES SIMPLEX VIRUS-1

Brian R. Bowman, Baylor College of Medicine, Texas.

Herpesviradae is a large family of viruses pathogenic to humans causing a variety of disorders ranging from cold sores and chicken pox to less frequent conditions such as blindness and cancers. Herpes Simplex Virus-1 (HSV-1) is the prototypical member of the herpesvirus family. The herpesvirus virion is a large virus containing a glycoprotein-containing envelope, a proteinaceous tegument layer, and a T=16 icosahedral nucleocapsid (diameter 120nm) encapsidating its double stranded DNA genome. VP5 (Mr 149kDa) is the major nucleocapsid protein present in 960 copies (150 hexons and 12 pentons) within the icosahedral lattice. VP5 and its subsequent substructures (hexons and pentons) are responsible for the formation of the capsid shell as well as for interactions with the tegument. A 65 kDa trypsin resistant fragment of this protein was identified (L451 - R1053), cloned, purified, and crystallized. The crystals belong to space group $P4_12_12$ with unit cell dimensions a=b=99.2 c=454.3 $\alpha=\beta=\chi=$ 90o. The structure was determined with MAD techniques and refined to 2.9 Å. The structure, the first for the major capsid protein from the herpesvirus family, revealed a novel fold, which with the combination of Cryo-EM and biochemical techniques was identified as the upper domain of VP5 (VP5ud). The VP5ud has an inherent flexibility in the number and types of interactions formed, allowing the VP5 subunits the leeway necessary to form both capsomeres, the pentons and hexons. The subunit rearrangements necessary to form the capsomeres result in structures that have completely different electrostatic properties. These differences have functional consequences important for the entry and release of the viral DNA.

Poster 56

ARP2/3 COMPLEX PROMOTES ACTIN FILAMENT ASSEMBLY AT THE LEADING EDGE OF MOTILE CELLS: INSIGHTS AT ATOMIC RESOLUTION.

Thomas D. Pollard. Molecular, Cellular and Developmental Biology, Yale University, New Haven CT.

Arp2/3 complex, a stable assembly of two actin-related proteins (Arp2 and Arp3) and five novel protein subunits, is the heart of the machine that generates the branched actin filament network responsible for pushing forward the leading edge of motile eukaryotic cells (Reviewed by Pollard et al., 2000). Our 2.0 Å resolution crystal structure of bovine Arp2/3 complex (Robinson/Turbedsy et al., 2001) confirmed that Arp2 and Arp3 are folded like actin with distinctive surface features. Subunits ARPC2 p34 and ARPC4 p20 in the core of the complex associate through long C-terminal alpha-helices and have similarly-folded N-terminal alpha/beta domains. ARPC1 p40 is a seven-blade beta-propeller with an insertion that may associate with the side of an actin filament. ARPC3 p21 and ARPC5 p16 are globular alpha-helical subunits. We predict that binding of WASp/Scar proteins activates Arp2/3 complex by bringing Arp2 into proximity with Arp3 for nucleation of a branch on the side of a pre-existing actin filament.

Arp2/3 complex promotes nucleation of actin filaments as 70° branches on the sides of older filaments. The complex is inactive until stimulated jointly by interaction with WASp/Scar proteins or other nucleation-promoting factors and with the side of a pre-existing filament. Total internal reflection fluorescence microscopy with rhodamine-labeled actin allowed us to observe polymerization in real time. In the presence of activated Arp2/3 complex, growing actin filaments form branches at random sites along their sides, rather than preferentially from their barbed ends (Amann and Pollard, 2001). The filament not only provides the base or "mother filament" for the branch but also acts as a secondary activator of nucleation. WASp/Scar proteins require activation through chemotactic signaling pathways, which guide the direction of cellular movement (Reviewed by Higgs and Pollard, 2001).

Amann, K.J. and Pollard, T.D. (2001) Direct real-time observation of actin filament branching mediated by Arp2/3 complex using total internal reflection microscopy. Proc. Nat. Acad. Sci. in press.

Higgs, N.H. and Pollard, T.D. (2001) Regulation of actin filament network formation through Arp2/3 complex: activation by a diverse array of proteins. Ann. Rev. Biochem. 70:649-676.

Pollard, T.D., Blanchoin, L. and Mullins, R.D. (2000) Biophysics of actin filament dynamics in nonmuscle cells. Ann. Rev. Biophys. Biomolec. Struct. 29:545-576.

Robinson*, R.C., Turbedsky*, K., Kaiser, D.A., Higgs, H.N., Marchand, J.-B., Choe, S. and Pollard, T.D. (2001) Crystal structure of Arp2/3 complex. Science 294:1679-1684. * co-first authors.

Poster 57

HIGH RESOLUTION IMAGING OF SINGLE PARTICLES IN A 300 KV LIQUID HELIUM ELECTRON CRYOMICROSCOPE

Zongli Li and Wah Chiu; National Center for Macromolecular Imaging, Baylor College of Medicine, One Baylor Plaza, Houston, TX 77030, USA

The Fujiyoshi type liquid helium electron cryomicroscope has been used successfully to image two-dimensional protein crystals and helical arrays in Japan. We have used the same type of instrument in Houston to image ice-embedded single particles. We initially encountered serious problems with the specimen charging. With the latest modification of the cryo-shield coupled with the procedures suggested by Unwin and Fujiyoshi, we begin to be able to record images of ice embedded single particles with detectable signals beyond 5 Å. The image contrast is similar for data recorded at either 4.2 or 75 K. We will demonstrate our current imaging results with the P22 phage particles (provided by Peter E. Prevelige at University of Alabama). We have found that the experimental B factor of our particle images is generally smaller than the equivalent data recorded with our former 400 kV cryomicroscope, with which we were able to reconstruct structures of icosahedral particles at 7 Å. This improvement will facilitate us to record images with higher signal to noise ratio aimed for reconstruction towards 4 Å.

AUTHOR & PAGE INDEX

Numbers refer to page in Study Guide.
"SP" before each number refers to Speaker Papers. "P" before numbers refers to posters.